977 ($M^+ - i$Pr). Second to elute (2*R*,5*S*,6*E*)-**23**: ^{1}H NMR ($CDCl_3$) δ 7.95 (dd, 1H, J = 7.5 Hz, J = 1.7 Hz), 7.71–7.56 (m, 3H), 7.41–7.30 (m, 5H), 7.15 (d, 2H, J = 8.5 Hz), 6.91 (d, 2H, J = 8.5 Hz), 5.58 (d, 1H, J = 8.0 Hz), 5.50 (dt, 1H, J_d = 15.8 Hz, J_t = 8.0 Hz), 5.36 (dd, 1H, J = 15.4 Hz, J = 5.1 Hz), 5.20 (t, 1H, J = 7.7 Hz), 5.01 (s, 2H), 3.92 (m, 2H), 3.71–3.63 (m, 7H), 3.54 (d, 1H, J = 4.9 Hz), 3.42 (d, 1H, J = 14.1 Hz), 3.05 (m, 2H), 2.93 (m, 1H), 2.67 (t, 2H, J = 7.5 Hz), 1.85 (m, 1H), 1.72 (m, 2H), 1.48 (m, 5H), 1.05 (m, 42H). MS (FAB$^+$) m/z 1021 (M^+), 977 ($M^+ - i$Pr).

(2*S*,5*S*,6*E*)-2,5-Bis[3-(triisopropylsilyloxy)propyl]-1-[3-(4-benzyloxyphenyl)propionyl]-7-(2-naphthylacetyl)-1,4,7-triazacycloundec-9-en-3-one [(2*S*,5*S*,6*E*)-30]. (2*S*,5*S*,6*E*)-**22** (612 mg, 0.6 mmol) was dissolved in DMF (6 ml) and was treated with mercaptoacetic acid (0.25 ml, 6 eq.) and $LiOH{\cdot}H_2O$ (280 mg, 11 eq.). The reaction was stirred for an hour at rt. The reaction was diluted in EtOAc and $NaHCO_3$. The aqueous layer was extracted twice with EtOAc. The combined organic layers were washed with brine, dried over $MgSO_4$ and concentrated. The product was used without further purification. It was dissolved in DMF (6 ml) and naphthylacetic acid (223 mg, 2 eq.) and HATU (456 mg, 2 eq.) were added. Et_3N (0.25 ml, 3 eq.) was then added dropwise and the reaction was stirred overnight at rt. Reaction was partitioned between ether and sat. $NaHCO_3$ solution. Aqueous phase was extracted 3× with ether. The combined organic phases were washed with water, brine, dried over $MgSO_4$ and concentrated. Purification by flash chromatography using hexane–EtOAc (70 : 30 to 65 : 35) furnished (2*S*,5*S*,6*E*)-**30** (382 mg, 63%): ^{1}H NMR ($CDCl_3$) δ for major rotamer 7.79 (m, 3H), 7.64 (s, 1H), 7.46–7.29 (m, 8H), 7.03 (d, 2H, J = 8.5 Hz), 6.89 (d, 2H, J = 8.7 Hz), 5.93 (d, 1H, J = 6.3 Hz), 5.43 (br d, 1H, J = 19.0 Hz), 5.03 (m, 3H), 4.31 (d, 1H, J = 13.7 Hz), 3.92–3.65 (m, 9H), 3.43–3.32 (m, 3H), 3.23 (dd, 1H, J = 10.7 Hz, J = 14.9 Hz), 2.79 (m, 2H), 2.48 (m, 1H), 2.28 (m, 1H), 1.98 (m, 1H), 1.73 (m, 1H), 1.54 (m, 3H), 1.36 (m, 3H), 1.03 (m, 42H). MS (FAB$^+$) m/z 1004 (M + H$^+$), 960 ($M^+ - i$-Pr); HRMS calcd for $C_{60}H_{90}N_3O_6Si_2^+$ (MH^+) 1004.6368, found 1004.6376.

(2*S*,5*S*,6*E*)-2,5-Bis(3-hydroxypropyl)-1-[3-(4-benzyloxyphenyl)-propionyl]-7-(2-naphthylacetyl)-1,4,7-triazacycloundec-9-en-3-one [(2*S*,5*S*,6*E*)-38]. (2*S*,5*S*,6*E*)-**30** (383 mg, 0.38 mmol) was dissolved in THF (3 ml) and was cooled down to −20 °C. TBAF solution (1M, 2 ml, 4 eq.) was added and the reaction was stirred for 48 h. TBAF solution (1M, 1 ml, 2 eq.) was added again and the reaction was stirred for 48 additional hours. The reaction was diluted with EtOAc and was quenched with water. The organic phase was washed twice with water. The combined aqueous phases were extracted 3× with EtOAc–hexane (9 : 1). The combined organic phases were washed with brine, dried over $MgSO_4$ and concentrated. Purification by flash chromatography using hexane–EtOAc (50 : 50), hexane–EtOAc–MeOH (48 : 48 : 4) and EtOAc–MeOH (92 : 8) furnished (2*S*,5*S*,6*E*)-**38** (206 mg, 78%): ^{1}H NMR ($CDCl_3$, 40 °C) δ 7.78 (m, 3H), 7.59 (s, 1H), 7.45–7.29 (m, 8H), 7.00 (d, 2H, J = 8.8 Hz), 6.87 (d, 2H, J = 8.5 Hz), 5.47 (m, 1H), 5.07 (m, 1H), 5.01 (s, 2H), 4.26 (d, 1H, J = 13.7 Hz), 3.83 (s, 2H), 3.77 (m, 2H), 3.61–3.50 (m, 5H), 3.31 (m, 3H), 3.20 (dd, 1H, J = 10.7 Hz, J = 14.1 Hz), 2.75 (m, 2H), 2.45 (m, 1H), 2.23 (m, 1H), 1.87 (m, 1H), 1.69–1.40 (m, 7H). MS (FAB$^+$) m/z 692 (M + H$^+$); HRMS calcd for $C_{42}H_{50}N_3O_6^+$ (MH^+) 692.3700, found 692.3712.

(2*S*,5*S*,6*E*)-2,5-Bis[(3-guanidino)propyl]-1-[3-(4-hydroxyphenyl)-propionyl]-7-(2-naphthylacetyl)-1,4,7-triazacycloundec-9-en-3-one [(2*S*,5*S*,6*E*)-54]. (2*S*,5*S*,6*E*)-**38** (150 mg, 0.22 mmol), PPh_3 (171 mg, 3 eq.) and *N*,*N*′-bis-Boc-guanidine (337 mg, 6 eq.) were added in a round-bottom flask and submitted to a vacuum/argon (3×). The products were dissolved in THF (3 ml) and the reaction was cooled down to 0 °C. DIAD solution (1.9M, 450 µl, 3.9 eq.) was added dropwise and the reaction was stirred for 24 h at rt. The reaction was partitioned between water and EtOAc. The organic phase was washed with brine, dried over $MgSO_4$ and concentrated. Purification by flash chromatography using hexane–EtOAc (70 : 30 to 30 : 70) furnished **46** (approx. 25 mg by NMR) as an inseparable mixture with Ph_3PO and mono-guanidylated product (166 mg). The mono-guanidylated product was resubmitted to Mitsunobu conditions and furnished **22** (approx. 47 mg by NMR) as an inseparable mixture with Ph_3PO. Mixtures of product **46** and Ph_3PO were dissolved in DCM (1.5 ml), treated with anisole (23 eq. based on approx. calculated mass) and pentamethylbenzene (34 eq.). TFA (4.5 ml) was added dropwise and the reaction was stirred for 8 h. The solvent was evaporated and oil was partitioned between water and ether. The water phase was lyophilized to give a yellowish foam which was purified by RP-HPLC in water–acetonitrile (90 : 10 to 40 : 60 in 33 min) to give (2*S*,5*S*,6*E*)-**54** (13 mg, 9%). MS (FAB$^+$) m/z 684 (M + H$^+$); HRMS calcd for $C_{37}H_{50}N_9O_4^+$ (MH^+) 684.3986, found 684.3984. $[\alpha]_D^{23}$ −51 (c = 0.1, AcOH).

Biological testing. Stable CHO cell transfectants expressing the CXCR4 variant were prepared as described previously.[35] CHO transfectants were harvested by treatment with citrate saline, and then washed in cold binding buffer (PBS containing 2 mg ml^{-1} BSA). For ligand binding, the cells were resuspended in binding buffer at 1 × 10^7 cells ml^{-1}, and 100 µL aliquots were incubated with 0.1 nM of [^{125}I]-SDF-1 (Perkin-Elmer Life Sciences) for 1 h on ice under constant agitation. Free and bound radioactivities were separated by centrifugation of the cells through an oil cushion, and bound radioactivity was measured with a gamma-counter (Cobra, Packard, Downers Grove, IL). The inhibitory activity of test compounds was determined based on the inhibition of [^{125}I]-SDF-1 binding to CXCR4 transfectants (IC50).

References

1 Y. Feng, C. C. Broder, P. E. Kennedy and E. A. Berger, *Science*, 1996, **272**, 872–877.
2 E. Oberlin, A. Amara, F. Bachelerie, C. Bessia, J. L. Virelizier, F. Arenzana-Seisdedos, O. Schwartz, J. M. Heard, I. Clark-Lewis, D. L. Legler, M. Loetscher, M. Baggiolini and B. Moser, *Nature*, 1996, **382**, 833–835.
3 H. Tamamura, A. Omagari, S. Oishi, T. Kanamoto, N. Yamamoto, S. C. Peiper, H. Nakashima, A. Otaka and N. Fujii, *Bioorg. Med. Chem. Lett.*, 2000, **10**, 2633.
4 N. Fujii, S. Oishi, K. Hiramatsu, T. Araki, S. Ueda, H. Tamamura, A. Otaka, S. Kusano, S. Terakubo, H. Nakashima, J. A. Broach, J. O. Trent, Z.-X. Wang and S. C. Peiper, *Angew. Chem., Int. Ed.*, 2003, **42**, 3251–3253.
5 H. Tamamura, Y. Xu, T. Hattori, X. Zhang, R. Arakaki, K. Kanbara, A. Omagari, A. Otaka, T. Ibuka, N. Yamamoto, H. Nakashima and N. Fujii, *Biochem. Biophys. Res. Commun.*, 1998, **253**, 877–882.

6 T. Murakami, A. Yoshida, R. Tanaka, S. Mitsuhashi, K. Hirose, M. Yanaka, N. Yamamoto and Y. Tanaka, *An orally bioavailable CXCR4 antagonist is a potent inhibitor of HIV-1 infection*. Presented at the 11th Conference on Retroviruses and Opportunistic Infections, San Francisco, USA, February 8–11, 2004, abstract 541.
7 G. A. Donzella, D. Schols, S. W. Lin, J. A. Este, K. A. Nagashima and P. J. Maddon, *Nat. Med.*, 1998, **4**, 72–76.
8 AMD3100 is now being developed as a potential new agent for stem cell transplants by Genzyme under the name Mozobil.
9 D. Schols, S. Claes, S. Hatse, K. Princen, K. De Vermeire, E. Clercq, R. Skerlj, G. Bridger and G. Calandra, *Anti-HIV activity profile of AMD070, an orally bioavailable CXCR4 antagonist H*. Presented at the 10th Conference on Retroviruses and Opportunistic Infections, Boston, MA, February 10–14, 2003, abstract 563.
10 D. Schols, S. Claes, S. Hatse, K. Princen, K. De Vermeire, E. Clercq, R. Skerlj, G. Bridger, G. Calandra, *Anti-HIV activity profile of AMD070, an orally bioavailable CXCR4 antagonist*. Presented at the 16th International Conference on Antiviral Research, Savannah, GA, April 27 to May 1, 2003, abstract A39, no. 2; D. Schols, S. Claes, S. Hatse, K. Princen, K. De Vermeire, E. Clercq, R. Skerlj, G. Bridger and G. Calandra, *Antiviral Res.*, 2003, **57**, 39.
11 B. Schmidt, C. Kühn, D. K. Ehlert, G. Lindeberg, S. Lindman, A. Karlén and A. Hallberg, *Bioorg. Med. Chem.*, 2003, **11**, 985–990.
12 (*a*) G. Dimartino, D. Wang, R. N. Chapman and P. S. Arora, *Org. Lett.*, 2005, **7**, 2389–2392; (*b*) I. N. Rao, A. Boruah, A. C. Kunwar, A. S. Devi, K. Vyas, K. Ravikumar and J. Iqbal, *J. Org. Chem.*, 2004, **69**, 2181–2184; (*c*) A. Boruah, I. N. Rao, J. P. Nandy, S. K. Kumar, A. C. Kunwar and J. Iqbal, *J. Org. Chem.*, 2003, **68**, 5006–5008.
13 (*a*) H. Tamamura, T. Araki, S. Ueda, Z. Wang, S. Oishi, A. Esaka, J. O. Trent, H. Nakashima, N. Yamamoto, S. C. Peiper, A. Otaka and N. Fujii, *J. Med. Chem.*, 2005, **48**, 3280–3289; (*b*) C. Ribera-Baeza, K. Kaljuste and A. Unden, *Neuropeptides*, 1996, **30**, 327.
14 A. Perdih and D. Kikelj, *Curr. Med. Chem.*, 2006, **13**, 1525–1556.
15 J. Cluzeau and W. D. Lubell, *Pept. Sci.*, 2005, **80**, 98–150.
16 S. Hanessian, G. McNaughton-Smith, H.-G. Lombart and W. D. Lubell, *Tetrahedron*, 1997, **53**, 12789–12854.
17 Y. Che and G. R. Marshall, *Biopolymers*, 2006, **81**, 392–406, and references therein.
18 Y. Sasaki, A. Niida, T. Tsuji, A. Shigenaga, N. Fujii and A. Otaka, *J. Org. Chem.*, 2006, **71**, 4969–4979, and references therein.
19 H. Tamamura, K. Hiramatsu, S. Ueda, Z. X. Wang, S. Kusano, S. Terakubo, J. O. Trent, S. C. Peiper, N. Yamamoto, H. Nakashima, A. Otaka and N. Fujii, *J. Med. Chem.*, 2005, **48**, 380–391.
20 (*a*) G. M. Dougherty, M. Jiménez and P. R. Hanson, *Tetrahedron*, 2005, **61**, 6218–6230; (*b*) S. Oishi, R. G. Karki, Z.-D. Shi, K. M. Worthy, L. Bindu, O. Chertov, D. Esposito, P. Frank, W. K. Gillette, M. Maderia, J. Hartley, M. C. Nicklaus, J. J. Barchi, Jr., R. J. Fisher and T. R. Burke, Jr., *Bioorg. Med. Chem.*, 2005, **13**, 2431–2438; (*c*) S. Oishi, Z.-D. Shi, K. M. Worthy, L. Bindu, R. J. Fisher and T. R. Burke, Jr., *ChemBioChem*, 2005, **6**, 668–674; (*d*) S. Rajesh, B. Banerji and J. Iqbal, *J. Org. Chem.*, 2003, **67**, 7852–7857.
21 A. Niida, H. Tanigaki, E. Inokuchi, Y. Sasaki, S. Oishi, H. Ohno, H. Tamamura, Z. Wang, S. C. Peiper, K. Kitaura, A. Otaka and N. Fujii, *J. Org. Chem.*, 2006, **71**, 3942–3951.
22 (*a*) R. Kaul, S. Surprenant and W. D. Lubell, *J. Org. Chem.*, 2005, **70**, 3838–3844; (*b*) C. J. Creighton, G. C. Leo, Y. Du and A. B. Reitz, *Bioorg. Med. Chem.*, 2004, **12**, 4375–4385; (*c*) T. Hoffmann, R. Waibel and P. Gmeiner, *J. Org. Chem.*, 2003, **68**, 62–69; (*d*) C. J. Creighton and A. B. Reitz, *Org. Lett.*, 2001, **3**, 893–895; (*e*) J. F. Reichwein and R. M. J. Liskamp, *Eur. J. Org. Chem.*, 2000, 2335–2344.
23 (*a*) E. Minta, C. Boutonnet, N. Boutard, J. Martinez and V. Rolland, *Tetrahedron Lett.*, 2005, **46**, 1795–1797; (*b*) M. Garcia, A. Serra, M. Rubiralta, A. Diez, V. Segarra, E. Lozoya, H. Ryder and J. M. Palacios, *Tetrahedron: Asymmetry*, 2000, **11**, 991–994; (*c*) K. Feichtinger, H. L. Sings, T. J. Baker, K. Matthews and M. Goodman, *J. Org. Chem.*, 1998, **63**, 8432–8439; (*d*) A. P. Nin, R. M. De Lederkremer and O. Varela, *Tetrahedron*, 1996, **52**, 12911–12918; (*e*) V. Mikol, C. Papageorgiou and X. Borer, *J. Med. Chem.*, 1995, **38**, 3361–3367.
24 G. Kokotos, *Synthesis*, 1990, 299–300.
25 S. Guttmann and R. A. Boissonnas, *Helv. Chim. Acta*, 1958, **41**, 1852–1867.
26 J. H. Cho and B. M. Kim, *Tetrahedron Lett.*, 2002, **43**, 1273–1276.
27 L. A. Carpino, *J. Am. Chem. Soc.*, 1993, **115**, 4397–4398.
28 D. L. Boger and D. Yohannes, *J. Org. Chem.*, 1988, **53**, 487–499.
29 S. Fustero, M. Sanchez-Rosello, D. Jimenez, J. F. Sanz-Cervera, C. Del Pozo and J. L. Acena, *J. Org. Chem.*, 2006, **71**, 2706–2714.
30 T. L. Suyama and W. H. Gerwick, *Org. Lett.*, 2006, **8**, 4541–4543.
31 RCM was done on a model system by cyclizing *N*-allyl-*N*-benzyl-3-butenamide. This compound was reported to react normally using Grubb's I in DCM and to give isomerized product using Grubb's II in refluxing toluene. In our hands, cyclisations were completed and we never observed any trace of isomerization product in the crude reaction mixtures, neither in DCM at 40 °C under argon, nor with addition of oxygen or PCy_3, or in refluxing toluene as reported in ref. 29. Grubb's II catalyst was purchased from Aldrich and used as supplied.

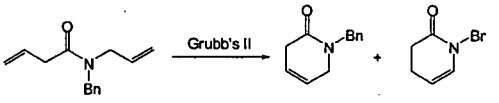

32 A. Pardi, M. Billeter and K. Wüthrich, *J. Mol. Biol.*, 1984, **180**, 741–751. Calculated using Karplus equation: $^3J_{HN-H\alpha} = 6.4 \times \cos^2(\theta - 60) - 1.4 \times \cos(\theta - 60) + 1.9$.
33 (*a*) R. Beumer and O. Reiser, *Tetrahedron*, 2001, **57**, 6497–6503; (*b*) F. Osterkamp, B. Ziemer, U. Koert, M. Wiesner, P. Raddatz and S. L. Goodman, *Chem.–Eur. J.*, 2000, **6**, 666–683; (*c*) D. S. Dodds and A. P. Kozikowski, *Tetrahedron Lett.*, 1994, **35**, 977–980.
34 H. Yoshino, M. Tsujii, M. Kodama, K. Komeda, N. Niikawa, T. Tanase, N. Asakawa, K. Nose and K. Yamatsu, *Chem. Pharm. Bull.*, 1990, **38**, 1735.
35 J. M. Navenot, Z. X. Wang, J. O. Trent, J. L. Murray, Q. X. Hu, L. DeLeeuw, P. S. Moore, Y. Chang and S. C. Peiper, *J. Mol. Biol.*, 2001, **59**, 380–393.

DOI: 10.1002/anie.200604342

Multicomponent Reactions

Direct Synthesis of 2-(Aminomethyl)indoles through Copper(I)-Catalyzed Domino Three-Component Coupling and Cyclization Reactions**

Hiroaki Ohno, Yusuke Ohta, Shinya Oishi, and Nobutaka Fujii**

The indole nucleus is a prominent structural motif found in numerous natural products and synthetic compounds with important biological activities, and thus considerable attention has been directed toward general, flexible, and selective methods for the synthesis of highly functionalized indole derivatives.[1] Among the functionalized indoles, the 2-(aminomethyl)indole motif is a key structure that exists in several biologically active compounds,[2] including calindol.[3] Most of the synthetic routes to 2-(aminomethyl)indoles rely upon functionalized indoles such as indole-2-carboxylic acid or its derivatives as the starting materials,[2-4] which limit the structure of the target molecules that can be readily synthesized.

One current important area of modern synthetic chemistry is the development of efficient practical methods that minimize the requisite reagents, solvents, cost, time, and separation processes for the desired transformation and also minimize the formation of waste.[5] While the multicomponent reaction (MCR) approach is recognized as a powerful method toward this end, a catalytic domino reaction including a MCR would be more attractive to achieve this goal. During the course of our efforts directed toward the development of useful transformations of allenic compounds,[6,7] we found that treatment of N-protected ethynylaniline **1a** with paraformaldehyde (**2**) and diisopropylamine (**3a**) in the presence of copper(I) bromide (Crabbé conditions)[8] gave 2-(aminomethyl)indole derivative **4a** in 92% yield (Scheme 1) without formation of the expected [2-(*N*-tosylamino)phenyl]allene. This reaction would proceed presumably through a Mannich-type MCR followed by formation of the indole ring from the plausible intermediate **7**. This is the first example of the formation of an indole ring system by a three-component reaction without producing any salts as by-products, although the synthesis of indole derivatives by catalytic domino three-component reactions including Sonogashira-type cross-coupling of dihalobenzenes[9] and haloanilines[10] were recently reported.[11] Herein we present a copper(I)-catalyzed domino three-component coupling–cyclization reaction of ethynylaniline derivatives with high atom economy to produce 2-(aminomethyl)indoles, with water as the waste product. Construction of polycyclic indole derivatives through this domino reaction and palladium-catalyzed C–H functionalization is also presented.

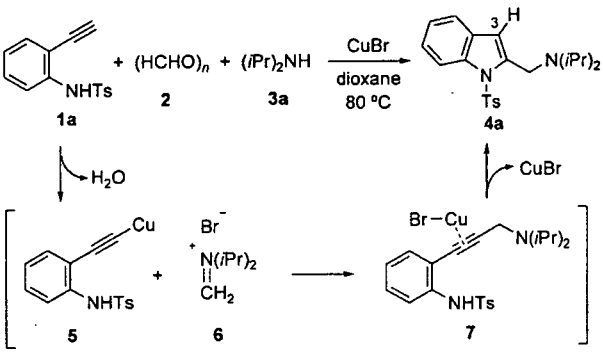

Scheme 1. Domino three-component coupling-indole formation. Ts = toluene-4-sulfonyl.

By modifying the original reaction conditions shown in Scheme 1 (CuBr, 1.0 equiv; (HCHO)$_n$, 2 equiv; and diisopropylamine, 3 equiv), we investigated the three-component formation of an indole ring under various reaction conditions (Table 1). To reduce the requisite amount of the amine

Table 1: Optimization of reaction conditions for the reaction with ethynylaniline **1a** and piperidine (**3b**).[a]

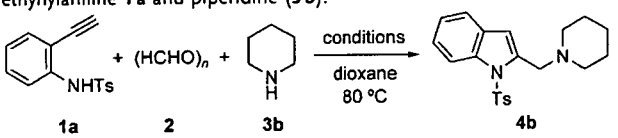

Entry	CuBr [mol%]	(HCHO)$_n$ [equiv]	Additive [equiv]	*t* [h]	Yield [%][b]
1	100	2.0	Et_3N [2.0]	0.25	71
2	10	2.0	Et_3N [2.0]	0.25	84
3	1	2.0	Et_3N [2.0]	0.25	92[c]
4	1	2.0	none	0.25	87
5	1	1.5	none	1	75
6	1	1.1	none	12	70

[a] Unless otherwise stated, reactions were carried out with **1** (0.18 mmol), (HCHO)$_n$ **2** (equivalents are shown in the Table), and piperidine (**3b**, 1.1 equiv) in 1,4-dioxane at 80°C. [b] Yields of isolated products. [c] The reaction was conducted on a 1.25-mmol scale.

[*] Dr. H. Ohno, Y. Ohta, Dr. S. Oishi, Prof. Dr. N. Fujii
Graduate School of Pharmaceutical Sciences
Kyoto University
Sakyo-ku, Kyoto 606-8501 (Japan)
Fax: (+81) 75-753-4570
E-mail: hohno@pharm.kyoto-u.ac.jp
nfujii@pharm.kyoto-u.ac.jp

[**] This work was supported in part by a Grant-in-Aid for the Encouragement of Young Scientists from the Ministry of Education, Culture, Sports, Science, and Technology of Japan, the 21st Century COE Program "Knowledge Information Infrastructure for Genome Science", the National Institute of Biomedical Innovation (Japan), and Meiji Seika, which are gratefully acknowledged.

component **3**, the reaction was first examined in the presence of Et_3N (2 equiv) using 1.1 equivalents of piperidine **3b**, which gave the expected indole **4b** in 71% yield (Table 1, entry 1). A catalytic reaction using 10 or 1 mol% of CuBr is also possible, and gives rise to **4b** in better yields (84–92%, Table 1, entries 2 and 3). In contrast, the reaction in the absence of any copper salt led to recovery of the starting material. The addition of Et_3N is not essential (entry 4), although the yield of **4b** was slightly decreased (87%). This result can be rationalized by the plausible mechanism depicted in Scheme 1, in which the sulfonamide proton is efficiently transferred to the 3-position of the indole nucleus. A decreased loading of $(HCHO)_n$ (1.5 or 1.1 equivalents) is also tolerated in this transformation, and leads to **4b** in yields of 75 and 70%, respectively (Table 1, entries 5 and 6); however, a longer reaction time (1–12 h) was required.

Next, the reaction of **1a** with various amines **3a–e** under the optimized conditions (Table 1, entry 4) was investigated. The results are summarized in Table 2. The reaction with the bulky diisopropylamine (**3a**, 1.1 equiv) and a catalytic amount of CuBr (1 mol%) resulted in **4a** in 81% yield. As well as piperidine (**3b**; Table 2, entry 2), pyrrolidine (**3c**) was also a good amine component in this reaction (89%, Table 2, entry 3). When a volatile amine such as diethylamine (**3d**) was used, the reaction proceeded well (89%) if it was used in increased amount (2 equiv, Table 2, entry 4). Secondary amines with removable benzyl groups **3e** also afforded the desired 2-[(*N*,*N*-dibenzylamino)methyl]indole **4e** in good yield (78%; Table 2, entry 5).

Table 2: Reaction with various amines.[a]

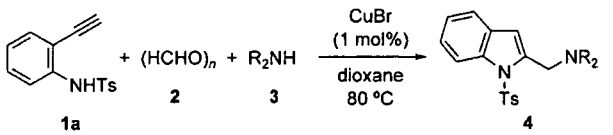

Entry	Amine **3**	*t* [h]	Product	R	Yield [%][b]
1	iPr_2NH (**3a**)	0.25	**4a**	*i*Pr	81
2	piperidine (**3b**)	0.25	**4b**	$R_2=(CH_2)_5$	87
3	pyrrolidine (**3c**)	0.25	**4c**	$R_2=(CH_2)_4$	89
4	Et_2NH (**3d**)[c]	0.25	**4d**	Et	89
5	Bn_2NH (**3e**)	2	**4e**	Bn	78

[a] Unless otherwise stated, reactions were carried out with **1a** (0.18 mmol), $(HCHO)_n$ **2** (2.0 equiv), amine **3** (1.1 equiv), and CuBr (1 mol%) in 1,4-dioxane at 80°C. [b] Yields of isolated products. [c] 2 equivalents of amine **3d** were used because of its volatility.

The reaction of various substituted components was then investigated. Anilines **1b** and **1c** bearing an electron-withdrawing methoxycarbonyl or trifluoromethyl group at the 3-position were allowed to react with dibenzylamine in the presence of a copper catalyst (1 mol%) to afford indoles **8** (79% yield) and **9** (61% yield), respectively (Table 3, entries 1 and 2). The reaction of **1d**, which has an electron-donating methyl group, also showed sufficient reactivity and gave indole **10** in 78% yield (Table 3, entry 3). This three-component cyclization is also applicable to the synthesis of 2-(aminomethyl)indoles having nitrogen-protecting groups other than the tosyl group: for example, *N*-(methoxycarbonyl)indole derivative **11** was prepared in 88% yield starting from ethynylaniline **1e** (Table 3, entry 4). The reaction is also possible with unsymmetrical secondary amines with functional groups: amine **3f** yielded indole **12** with a bromine atom on the benzene ring in 80% yield (Table 3, entry 5) without causing any undesired side reactions.

Table 3: Reaction of variously substituted components.[a]

Entry	Ethynylaniline	Amine	conditions	Product (yield)[b]
1	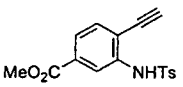 **1b**	Bn_2NH, **3e**	80°C, 5 h	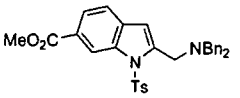 **8** (79%)
2	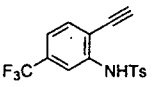 **1c**	Bn_2NH, **3e**	80°C, 3 h	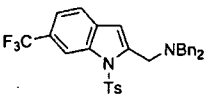 **9** (61%)
3	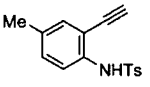 **1d**	Bn_2NH, **3e**	80°C, 5 h then reflux, 1 h	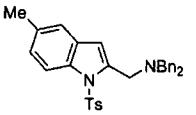 **10** (78%)
4	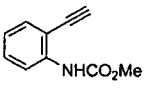 **1e**	 **3b**	80°C, 15 min	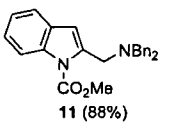 **11** (88%)
5	**1a**	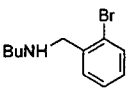 **3f**	80°C, 3 h then reflux, 1 h	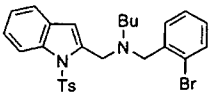 **12** (80%)

[a] All reactions were carried out with **1** (0.18 mmol), $(HCHO)_n$ **2** (2.0 equiv), amine **3** (1.1 equiv), and CuBr (1 mol%) in 1,4-dioxane. [b] Yields of isolated products.

The polycyclic indole is an important core framework for biologically active compounds.[12] Therefore, the development of an efficient method for the construction of this framework is strongly required.[13] We expected that the newly developed three-component reaction for the formation of an indole ring would serve as an extremely useful synthetic route to this class of compounds. We thus investigated the construction of polycyclic indole skeletons by a sequential three-component reaction leading to the formation of an indole ring followed by a palladium-catalyzed functionalization of a C–H bond. As shown in Scheme 2, the formation of an indole ring system

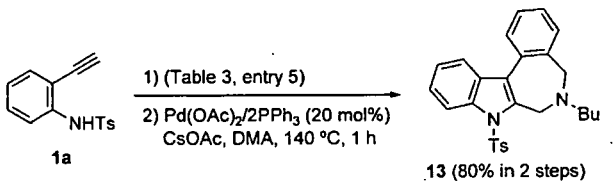

Scheme 2. Construction of a polycyclic indole structure by a three-component reaction and palladium-catalyzed cyclization. DMA = dimethylacetamide.

from N-protected ethynylaniline **1a** (Table 3, entry 5) and, after purification, subsequent palladium-catalyzed cyclization of the resulting 2-(aminomethyl)indole **12** gave the desired dihydrobenzoazepine-fused indole **13** in 80% yield over the two steps.

In conclusion, we have developed a novel domino three-component coupling reaction for the synthesis of 2-(aminomethyl)indoles and polycyclic indole derivatives. This study has resulted in the first catalytic multicomponent construction of an indole ring that produces water as the only theoretical by-product. This domino reaction, in which two carbon–nitrogen bonds and one carbon–carbon bond are formed, is synthetically useful since functionalized 2-(aminomethyl)indoles and their polycyclic derivatives can be obtained directly from readily available N-protected ethynylanilines.

Experimental Section

General procedure for three-component formation of an indole: Piperidine (**3b**; 20.0 μL, 0.20 mmol) was added at room temperature under Ar to a stirred suspension of N-tosylated ethynylaniline **1a** (50 mg, 0.18 mmol), paraformaldehyde (**2**; 11.1 mg, 0.37 mmol), and CuBr (0.26 mg, 0.0018 mmol) in dioxane. After stirring the mixture for 15 min at 80 °C, it was concentrated under reduced pressure and purified by column chromatography over silica gel with hexane/EtOAc (5:1) as the eluent to afford the desired product **4b** (59.2 mg, 87%) as a colorless oil: IR: $\tilde{\nu}$ = 1367 (NSO_2), 1173 cm^{-1} (NSO_2); ^1H NMR (400 MHz, $CDCl_3$): δ = 1.42–1.49 (m, 2H, CH_2), 1.50–1.58 (m, 4H, 2 × CH_2), 2.33 (s, 3H, Ph*Me*), 2.44-2.54 (m, 4H, 2 × NCH_2), 3.84 (s, 2H, 1'-CH_2), 6.54 (s, 1H, 3-H), 7.18 (d, J = 8.4 Hz, 2H, Ar), 7.25 (ddd, J = 7.4, 7.4, 1.1 Hz, 1H, Ar), 7.17–7.20 (m, 1H, Ar), 7.44 (d, J = 7.4 Hz, 1H, Ar), 8.03 (d, J = 8.4 Hz, 2H, Ar), 8.07 ppm (d, J = 8.3 Hz, 1H, Ph); ^{13}C NMR (100 MHz, $CDCl_3$): δ = 21.5, 24.3, 25.9 (2C), 54.6, 56.1 (2C), 111.2, 114.5, 120.4, 123.2, 124.0, 127.2 (2C), 129.0, 129.4 (2C), 136.5, 137.0, 138.4, 144.4 ppm; MS (FAB) *m/z* (%): 369 (100); HRMS (FAB) calcd for $C_{21}H_{25}N_2O_2S$ [M+H$^+$]: 369.1637; found: 369.1632.

Synthesis of polycyclic indole **13** by palladium-catalyzed functionalization of the C–H bond: $Pd(OAc)_2$ (4.3 mg, 0.019 mmol), PPh_3 (10 mg, 0.038 mmol), and CsOAc (36 mg, 0.19 mmol) were added to a stirred solution of **12** (50 mg, 0.095 mmol) at room temperature under Ar. After stirring the mixture for 1 h at 140 °C, it was concentrated under reduced pressure and purified by column chromatography over silica gel with hexane/AcOEt (4:1) as the eluent to afford the desired product **13** (42 mg, quant.) as a colorless oil: IR: $\tilde{\nu}$ = 1374 (NSO_2), 1174 cm^{-1} (NSO_2); ^1H NMR (400 MHz, $CDCl_3$): δ = 0.98 (t, J = 7.2 Hz, 3H, CH_3), 1.39–1.49 (m, 2H, CH_3CH_2), 1.61–1.68 (m, 2H, $CH_2CH_2CH_2$), 2.30 (s, 3H, Ph*Me*), 2.67 (t, J = 7.2 Hz, 2H, NCH_2CH_2), 3.42 (s, 2H, NCH_2), 4.05 (s, 2H, NCH_2), 7.16 (d, J = 8.8 Hz, 2H, Ar), 7.23–7.45 (m, 5H, Ar), 7.67 (d, J = 6.1 Hz, 1H, Ar), 7.73 (d, J = 7.6 Hz, 1H, Ar), 7.83 (d, J = 8.4 Hz, 2H, Ar), 8.57 ppm (d, J = 8.4 Hz, 1H, Ar); ^{13}C NMR (100 MHz, $CDCl_3$): δ = 14.1, 20.6, 21.5, 30.1, 47.9, 55.8, 56.2, 115.6, 119.3, 123.8, 124.0, 124.8, 126.7 (2C), 127.2, 127.4, 127.5, 128.0, 129.7 (2C), 130.6, 134.4, 135.4 (2C), 137.0, 137.0, 144.7 ppm; MS (FAB) *m/z* (%): 445 (100); HRMS (FAB) calcd for $C_{27}H_{29}N_2O_2S$ [MH^+]: 445.1950; found: 445.1952.

Received: October 24, 2006
Published online: February 15, 2007

Keywords: cyclization · domino reactions · homogeneous catalysis · indoles · multicomponent reactions

[1] For recent reviews, see: a) G. R. Humphrey, J. T. Kuethe, *Chem. Rev.* **2006**, *106*, 2875–2911; b) S. Cacchi, G. Fabrizi, *Chem. Rev.* **2005**, *105*, 2873–2920.

[2] For recent examples, see: a) J. A. Morón, M. Campillo, V. Perez, M. Unzeta, L. Pardo, *J. Med. Chem.* **2000**, *43*, 1684–1691; b) G. Spadoni, C. Balsamini, G. Diamantini, A. Tontini, G. Tarzia, *J. Med. Chem.* **2001**, *44*, 2900–2912; c) S. Rivara, M. Mor, C. Silva, V. Zuliani, F. Vacondio, G. Spadoni, A. Bedini, G. Tarzia, V. Lucini, M. Pannacci, F. Fraschini, P. V. Plazzi, *J. Med. Chem.* **2003**, *46*, 1429–1439; d) A. O. Stewart, M. D. Cowart, R. B. Moreland, S. P. Latshaw, M. A. Matulenko, P. A. Bhatia, X. Wang, J. F. Daanen, S. L. Nelson, M. A. Terranova, M. T. Namovic, D. L. Donnelly-Roberts, L. N. Miller, M. Nakane, J. P. Sullivan, J. D. Brioni, *J. Med. Chem.* **2004**, *47*, 2348–2355; e) S. Rivara, S. Lorenzi, M. Mor, P. V. Plazzi, G. Spadoni, A. Bedini, G. Tarzia, *J. Med. Chem.* **2005**, *48*, 4049–4060; f) M. Brands, J.-K. Ergüden, K. Hashimoto, D. Heimbach, C. Schröder, S. Siegel, J.-P. Stasch, S. Weigand, *Bioorg. Med. Chem. Lett.* **2005**, *15*, 4201–4205.

[3] a) A. Kessler, H. Faure, C. Petrel, M. Ruat, P. Dauban, R. J. Dodd, *Bioorg. Med. Chem. Lett.* **2004**, *14*, 3345–3349; b) C. Petrel, A. Kessler, P. Dauban, R. H. Dodd, D. Rognan, M. Ruat, *J. Biol. Chem.* **2004**, *279*, 18990–18997; c) K. Ray, J. Tisdale, R. H. Dodd, P. Dauban, M. Ruat, J. K. Northup, *J. Biol. Chem.* **2005**, *280*, 37013–37020.

[4] For recent synthesis of 2-(aminomethyl)indoles by other approaches, see: a) I. Ambrogio, S. Cacchi, G. Fabrizi, *Org. Lett.* **2006**, *8*, 2083–2086; b) M. S. C. Pedras, M. Suchy, P. W. K. Ahiahonu, *Org. Biomol. Chem.* **2006**, *4*, 691–701.

[5] B. M. Trost, *Acc. Chem. Res.* **2002**, *35*, 695–705.

[6] a) H. Ohno, K. Miyamura, Y. Takeoka, T. Tanaka, *Angew. Chem.* **2003**, *115*, 2751–2754; *Angew. Chem. Int. Ed.* **2003**, *42*, 2647–2650; b) H. Ohno, K. Miyamura, T. Mizutani, Y. Kadoh, Y. Takeoka, H. Hamaguchi, T. Tanaka, *Chem. Eur. J.* **2005**, *11*, 3728–3741; c) H. Ohno, T. Mizutani, Y. Kadoh, K. Miyamura, T. Tanaka, *Angew. Chem.* **2005**, *117*, 5243–5245; *Angew. Chem. Int. Ed.* **2005**, *44*, 5113–5115; d) H. Ohno, Y. Kadoh, N. Fujii, T. Tanaka, *Org. Lett.* **2006**, *8*, 947–950.

[7] For recent reviews, see: a) H. Ohno, *Chem. Pharm. Bull.* **2005**, *53*, 1211–1226; b) H. Ohno, *Yakugaku Zasshi* **2005**, *125*, 899–925.

[8] S. Searles, Y. Li, B. Nassim, M.-T. R. Lopes, P. T. Tran, P. Crabbé, *J. Chem. Soc. Perkin Trans. 1* **1984**, 747–751.

[9] a) L. Ackermann, *Org. Lett.* **2005**, *7*, 439–442; b) L. T. Kaspar, L. Ackermann, *Tetrahedron* **2005**, *61*, 11311–11316.

[10] a) N. Olivi, P. Spruyt, J.-F. Peyrat, M. Alami, J.-D. Brion, *Tetrahedron Lett.* **2004**, *45*, 2607–2610; b) B. Z. Lu, W. Zhao, H.-X. Wei, M. Dufour, V. Farina, C. H. Senanayake, *Org. Lett.* **2006**, *8*, 3271–3274.

[11] For a two-component indole synthesis by a Sonogashira-type reaction, see: a) S. Cacchi, G. Fabrizi, L. M. Parisi, *Org. Lett.* **2003**, *5*, 3843–3846; b) M. McLaughlin, M. Palucki, I. W. Davies, *Org. Lett.* **2006**, *8*, 3307–3310.

[12] For biologically active polycyclic indoles with a 2-(aminomethyl)moiety, see: a) A. Espada, C. Jiménez, C. Debitus, R. Riguera, *Tetrahedron Lett.* **1993**, *34*, 7773–7776; b) M. A. Rashid, K. R. Gustafson, M. R. Boyd, *J. Nat. Prod.* **2001**, *64*, 1454–1456; c) R. A. Glennon, B. Grella, R. J. Tyacke, A. Lau, J. Westaway, A. L. Hudson, *Bioorg. Med. Chem. Lett.* **2004**, *14*, 999–1002; d) C. Liu, M. N. Masuno, J. B. MacMillan, T. F. Molinski, *Angew. Chem.* **2004**, *116*, 6077–6080; *Angew. Chem. Int. Ed.* **2004**, *43*, 5941–5945; e) R. N. Sonnenschein, J. J. Farias, K. Tenney, S. L. Mooberry, E. Lobkovsky, J. Clardy, P. Crews, *Org. Lett.* **2004**, *6*, 779–782.

[13] For recent synthesis of polycyclic indoles, see a) H. Kusama, J. Takaya, N. Iwasawa, *J. Am. Chem. Soc.* **2002**, *124*, 11592–11593; b) M. Bandini, A. Melloni, F. Piccinelli, R. Sinisi, S. Tommasi, A. Umani-Ronchi, *J. Am. Chem. Soc.* **2006**, *128*, 1424–1425; c) N. Kuroda, Y. Takahashi, K. Yoshinaga, C. Mukai, *Org. Lett.* **2006**, *8*, 1843–1845.

JOURNAL OF VIROLOGY, Jan. 2008, p. 588–592 Vol. 82, No. 1
0022-538X/08/$08.00+0 doi:10.1128/JVI.01697-07

Heptad Repeat-Derived Peptides Block Protease-Mediated Direct Entry from the Cell Surface of Severe Acute Respiratory Syndrome Coronavirus but Not Entry via the Endosomal Pathway▽

Makoto Ujike,[1]† Hiroki Nishikawa,[2]† Akira Otaka,[3] Naoki Yamamoto,[4] Norio Yamamoto,[4] Masao Matsuoka,[5] Eiichi Kodama,[5] Nobutaka Fujii,[2,5]* and Fumihiro Taguchi[1]*

Department of Virology III, National Institute of Infectious Disease, Gakuen 4-7-1, Musashi-murayama, Tokyo 208-0011, Japan[1]; Graduate School of Pharmaceutical Sciences, Kyoto University, Sakyo-ku, Kyoto 606-8501, Japan[2]; Graduate School of Pharmaceutical Sciences, The University of Tokushima, Tokushima 770-8505, Japan[3]; Department of Molecular Virology, Tokyo Medical and Dental University, 1-5-45 Yushima, Bunkyo-ku, Tokyo 113-8519, Japan[4]; and Institute for Virus Research, Kyoto University, Sakyo-ku, Kyoto 606-8507, Japan[5]

Received 6 August 2007/Accepted 6 October 2007

The peptides derived from the heptad repeat (HRP) of severe acute respiratory syndrome coronavirus (SCoV) spike protein (sHRPs) are known to inhibit SCoV infection, yet their efficacies are fairly low. Recently our research showed that some proteases facilitated SCoV's direct entry from the cell surface, resulting in a more efficient infection than the previously known infection via endosomal entry. To compare the inhibitory effect of the sHRP in each pathway, we selected two sHRPs, which showed a strong inhibitory effect on the interaction of two heptad repeats in a rapid and virus-free in vitro assay system. We found that they efficiently inhibited SCoV infection of the protease-mediated cell surface pathway but had little effect on the endosomal pathway. This finding suggests that sHRPs may effectively prevent infection in the lungs, where SCoV infection could be enhanced by proteases produced in this organ. This is the first observation that HRP exhibits different effects on virus that takes the endosomal pathway and virus that enters directly from the cell surface.

Severe acute respiratory syndrome (SARS) coronavirus (SCoV) is a causative agent of life-threatening SARS (4, 7, 15, 31). Although the first outbreak of SARS was stamped out, an effective antiviral drug is still required for the treatment and prevention of possible future outbreaks. SCoV is an enveloped virus and enters cells via fusion between the cellular membrane and its envelope. SCoV membrane fusion is mediated by the spike (S) protein, which is classified as a class I fusion protein. One of the most important features of class I fusion proteins is the conserved heptad repeat regions (HR1 and HR2) which play an essential role in virus-cell fusion activities (3, 6, 10, 28). In the fusion process, HR1 forms an interior, trimeric coiled-coil structure to which HR2 binds in an antiparallel fashion, resulting in the formation of a six-helix bundle. This structure brings viral and cellular membranes into close proximity to facilitate membrane fusion. Synthetic short peptides derived from the HR (HRP) of class I fusion proteins have been shown to block the interaction of HR1-HR2 complexes, resulting in the inhibition of a number of viral infections, including those of retroviruses (11, 14, 21, 23, 32, 38, 39), paramyxoviruses (12, 16, 30, 36, 42–44), filovirus (37), and coronavirus (2). Similarly, HRP of SCoV S (sHRP) could also inhibit SCoV and human immunodeficiency virus (HIV)/SCoV-pseudotyped virus infection (1, 18, 24, 45). However, these inhibitory effects were significantly less than those of one of the most effective HRPs from HIV type 1 (HIV-1) (39) and even those from the same family, murine coronavirus mouse hepatitis virus (MHV) (2).

The major organs targeted by SCoV are the lungs and intestines, although the virus grows in a variety of tissues that express angiotensin-converting enzyme 2 (ACE2). Recently we and others showed that SCoV uses two distinct entry pathways depending on the presence of proteases (20, 33, 34). In the absence of proteases, SCoV enters the cell via an endosomal pathway (9, 26, 41), with the S protein activated for fusion by the cathepsin L protease, which is active only under acidic conditions in the endosome (8, 33). In contrast, in the presence of protease, SCoV virion S proteins attach to ACE2 on the host cell surface and are activated for fusion by proteases such as trypsin or elastase, which leads to envelope-plasma membrane fusion and direct entry from the cell surface (20, 33, 34). Infection via the cell surface is more than 100 times more efficient than infection via the endosomal pathway (20). These results suggested the possibility that the severe illnesses in the lung and intestine could be due to the enhancement of direct SCoV cell surface entry mediated by proteases produced in these organs (20).

Although previous studies have described the inhibitory effects of the sHRP on SCoV infection via the endosomal path-

* Corresponding author. Mailing address for F. Taguchi: Department of Virology III, National Institute of Infectious Disease, Gakuen 4-7-1, Musashi-murayama, Tokyo 208-0011, Japan. Phone: 81-42-561-0771, ext. 533. Fax: 81-42-567-5631. E-mail: ftaguchi@nih.go.jp. Mailing address for N. Fujii: Graduate School of Pharmaceutical Sciences, Kyoto University, Sakyo-ku, Kyoto 606-8501, Japan. Phone: 81-75-753-4511. Fax: 81-75-753-4570. E-mail: nfujii@pharm.kyoto-u.ac.jp.
† M.U. and H.N. contributed equally to this work.
▽ Published ahead of print on 17 October 2007.

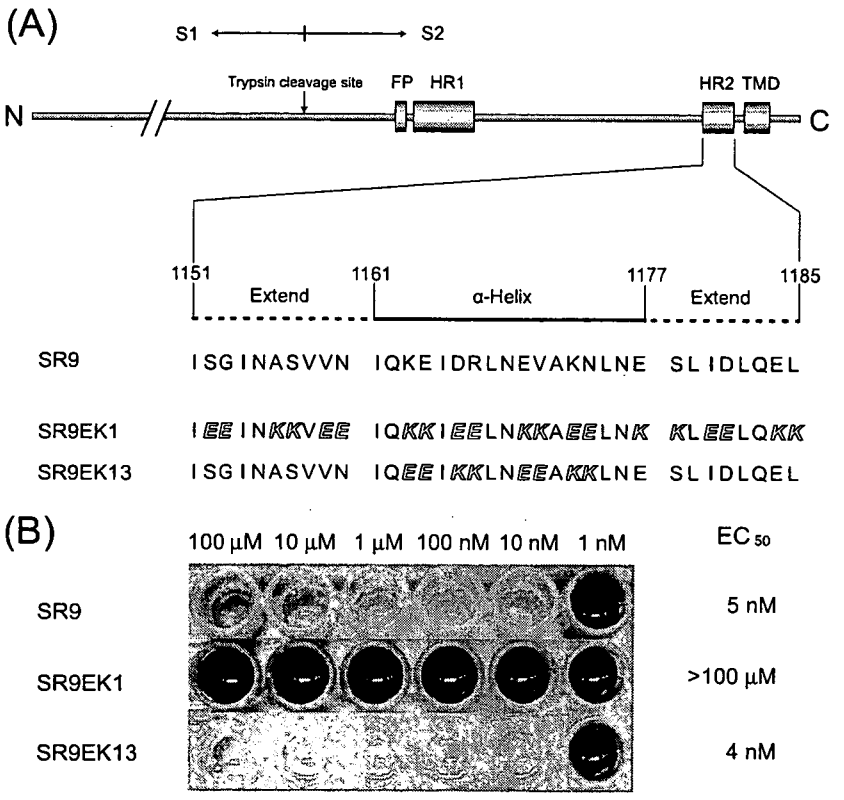

FIG. 1. (A) Schematic of SCoV S protein and sequences of native sHRP (SR9) and its EK substitution derivatives. The S protein contains two α-helical heptad repeats (HR1 and HR2), a putative fusion peptide (FP), a transmembrane domain (TMD), and a trypsin cleavage site (17). The expanded region shows the amino acid sequence of HR2 (SR9), which consists of two extended parts (1151 to 1160 and 1178 to 1185) and one α-helix part (1161 to 1177). Substituted EKs are shown with italic white letters. (B) In vitro binding inhibition assay of HRPs. GST-HR2-coated plates were incubated with MBP-HR1 in the presence of various concentrations (1 nM to 100 μM) of sHRP. Inhibitory potency of the peptide was assessed using the anti-MBP antibody-alkaline phosphatase conjugate and staining with 5-bromo-4-chloro-3-indolylphosphate.

way (1, 18, 24, 45), little is known about their effects on the protease-mediated cell surface pathway. Thus, in this study, we reevaluated the inhibitory effects of the sHRP on infection via the two distinct pathways of SCoV entry.

Recent studies of the X-ray crystal structure of the SCoV S HR1-HR2 complex have shown that the HR2 peptide consists of two extended regions and one α-helical region (35, 40). Since we have found that HRPs with replacement by the X-EE-XX-KK sequence in the HIV-1 HR2 region exhibited potent anti-HIV-1 activity (27), we chose to modify the α-helical region of HRP derived from SCoV S HR2 (sHRP) and also to prepare the control peptide SR9EK1 without sequence relatedness (Fig. 1A). To estimate these sHRPs, we established a rapid and virus-free in vitro novel assay system based on the inhibition of HR1-HR2 complex formation. Two fusion proteins (maltose binding protein [MBP]-HR1 [amino acid residues of the S protein, 892 to 964] and glutathione *S*-transferase [GST]-HR2 [1141 to 1192]) were expressed using *Escherichia coli* and purified using amylose resin (New England Biolabs) and glutathione Sepharose 4B (GE Healthcare, Bucks, United Kingdom), respectively. An enzyme-linked immunosorbent assay plate was coated with GST-HR2 dissolved in sodium carbonate buffer (pH 8.5), 3.6 μg/ml in concentration, by incubation at 4°C for 8 h. After bovine serum albumin blocking (1 mg/ml) at 4°C for 2.5 h, GST-HR2 on the plate was allowed to bind the MBP-HR1 protein (8.8 μg/ml) by incubation at 37°C for 1.5 h in the presence of various concentrations of sHRPs to be examined for inhibition activity. After the plate was washed, the inhibiting potency of the peptide was assessed by colorimetric analyses using the anti-MBP antibody-alkaline phosphatase conjugate (Sigma) with a 1:1,000 dilution with incubation at 4°C for 1 h and then staining with BluePhos microwell phosphatase (KPL). As shown in Fig. 1B, SR9 and SR9EK13 showed significant binding inhibition in a nanomolar range, whereas the control, SR9EK1, without sequence relatedness, had no inhibitory effect at a concentration of 100 μM.

We tested the inhibitory effects of SR9 and SR9EK13 on SCoV entry, since these sHRPs were found to have a strong binding inhibition activity, along with the control peptide SR9EK1. We examined their effects on both the endosomal and protease-mediated cell surface entry processes. Viral entry via the endosome was examined as described previously with a slight modification (20). In brief, VeroE6 cells were pretreated with each sHRP at 37°C for 30 min and then inoculated with SCoV (multiplicity of infection = 1.0) and incubated on ice for 30 min to allow viral attachment to ACE2 but not viral entry. After removal of unattached viruses, the cells were incubated at 37°C for 6 h. Viral entry was measured by quantifying the newly synthesized mRNA9 using real-time PCR (20). To evaluate entry via the cell surface, the cells were pretreated with 1

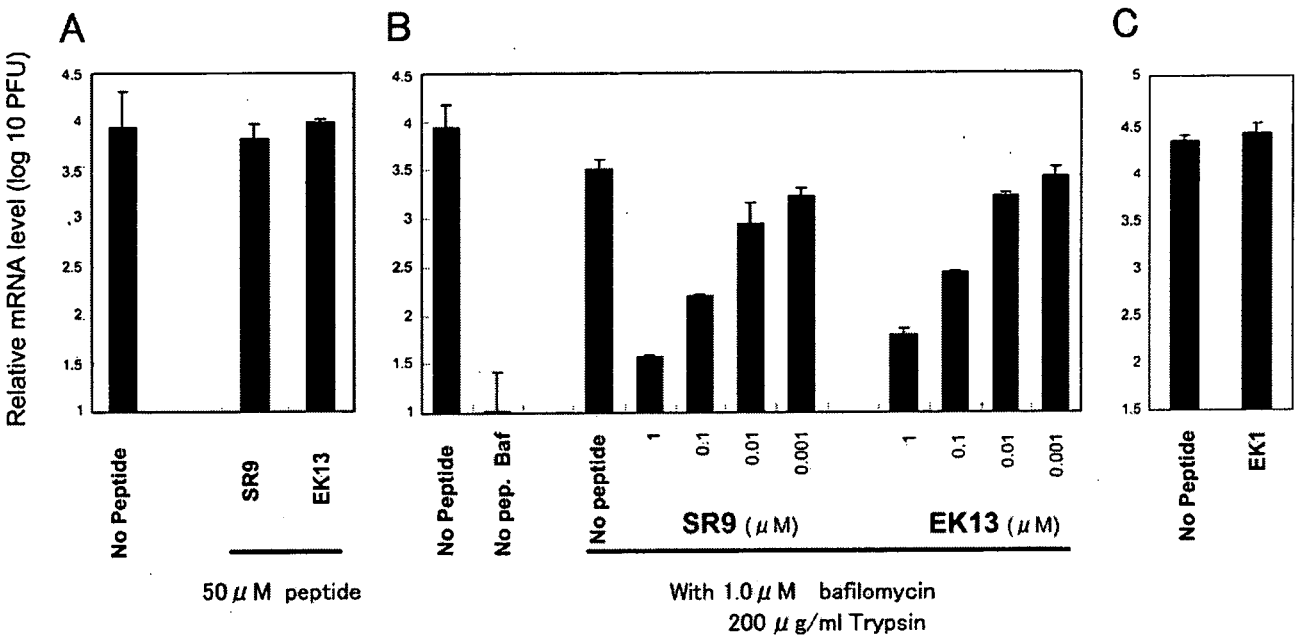

FIG. 2. Inhibitory effect of sHRPs on SCoV infections via the endosomal pathway (A) or protease-mediated cell-surface pathway (B). (A) VeroE6 cells were pretreated with 50 μM sHRPs at 37°C for 30 min, placed on ice for 10 min, and then inoculated with SCoV at a multiplicity of infection of 1.0 on ice for 30 min. After the removal of unbound virus, the cells were incubated in medium containing 50 μM sHRPs at 37°C for 6 h. (B) Cells pretreated with 1 μM Baf and sHRPs at the indicated concentrations were inoculated with SCoV as described above. After the removal of unbound virus, the cells were treated with 200 μg/ml L-1-tosylamide-2-phenylethyl chloromethyl ketone-treated trypsin at room temperature for 5 min and incubated at 37°C for 6 h. sHRP and Baf were present in the media in all steps at indicated concentrations. To measure amounts of viruses that entered cells, cells were infected with 10-fold-stepwise-diluted SARS-CoV from 10^6 to 10^2 PFU without Baf and trypsin and the amounts of mRNA9 were quantified by real-time PCR. Amounts of viral entry in this study were calculated from a calibration line obtained as described above and are shown as relative mRNA levels (20). (C) EK1 has no sequential similarity to sHRP and showed no inhibitory effect in vitro. Cells were treated with 1 μM EK1 as a control peptide, and other procedures were performed as described for panel B.

μM bafilomycin (Baf), which blocks SCoV endosomal entry, at 37°C for 30 min before SCoV inoculation. After removal of unattached viruses, the cells were treated with trypsin (0.2 mg/ml) for 5 min at room temperature and viral entry was measured as described above. Each sHRP and/or Baf was present in the media in all steps at various concentrations. In the absence of proteases, these sHRPs showed no measurable inhibitory effect on SCoV endosomal infection even at concentrations as high as 50 μM, despite showing a potent inhibitory effect in vitro (Fig. 2A). This lack of inhibition is consistent with previous observations that the same or homologous-sequence sHRPs had no inhibitory effect on SCoV infection at high concentrations of 10 μM (45) or 50 μM (1), respectively. In contrast, when SCoV was allowed to enter cells via the cell surface by treatment with protease and Baf, these sHRPs showed a strong inhibitory effect on SCoV infection in a dose-dependent manner (Fig. 2B). At a concentration of 0.1 μM, the SR9 sHRP reduced newly synthesized mRNA9 levels by about 10-fold, while an sHRP concentration of 1 μM saw a 50-fold decrease. The control sHRP, SR9EK1, did not inhibit SCoV cell-surface-mediated infection even at the concentration of 1 μM, indicating that the inhibition is peptide sequence specific (Fig. 2C). We finally evaluated the inhibitory effect of sHRPs in the presence of trypsin but without Baf treatment. These conditions may resemble the situation of patients with severe SARS, in which some proteases were produced in the infected lung and intestinal tissue. Under these conditions, these sHRPs also showed a potent inhibitory effect on SCoV infection (Fig. 3).

The present study indicates that our sHRPs fail to inhibit endosome-mediated SCoV infection. This finding is consistent with those of previous studies indicating that sHRPs have a low inhibitory effect on endosomal infection of native SCoV. The reported 50% effective dose (EC_{50}) was 3.68 to 19.0 μM (1, 18, 45). However, our results suggest that sHRPs, which showed no measurable inhibitory effect on SCoV endosomal infection, have a very strong inhibitory effect on protease-mediated cell surface SCoV infection; the EC_{50} was less than 100 nM (Fig. 2B and 3). Cell surface infection of SCoV is anticipated to occur in the lungs of SARS patients, since various types of inflammatory cells infiltrate the lung of the patients (25), and thus elastase, a protease produced in lung inflammation (13) and shown to enhance SCoV infection in cultured cells (20), could enhance SCoV infection in the lung by facilitating the infection from cell surface. Inhibitory effects of sHRPs on cell surface infection may help prevent severe damage by SCoV infection in the major target organ. Thus, the sHRPs shown in this study would be effective anti-SARS therapeutic drugs.

A few possibilities are conceivable for the explanation of an inefficient inhibitory effect of sHRPs in infection via the endosomal pathway. One is the failure of sHRPs to be trafficked to the endosome vehicles from culture medium. Thus, their concentration in the endosome is not sufficient to prevent SCoV infection. Alternatively, sHRPs may be sufficiently transported

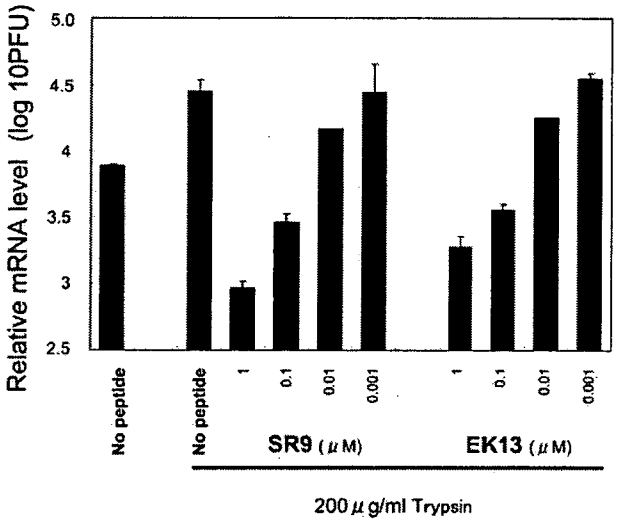

FIG. 3. Effective inhibition by HRPs of SCoV infection in the presence of exogenous trypsin. VeroE6 cells pretreated with sHRPs at the indicated concentrations were inoculated with SCoV as described in the legend to Fig. 2. After the removal of unbound virus, the cells were treated with 200 μg/ml L-1-tosylamide-2-phenylethyl chloromethyl ketone-treated trypsin at room temperature for 5 min and incubated at 37°C for 6 h. sHRPs were present in the media in all steps at the indicated concentrations. The relative viral mRNA9 was measured quantitatively by real-time PCR as described in the legend to Fig. 2. In this assay, cells were not treated with Baf throughout the experiment.

to the endosome but are inactivated by the low-pH environment or are degraded or digested with proteases present in the endosome. Another possibility is that the conformation of the cleaved S protein in the acidic environment of the endosome is different from that in a neutral pH and the sHRP fails to bind to the S protein in the former environment even if six-helix bundles with intramolecular HR2 are formed under both conditions. We are currently studying whether the inefficient inhibition of virus entry into cells could be attributed to one of those possibilities, or even another.

Interestingly, the EC_{50} (approximately 680 μM) of HRP of Ebola virus (37), which is thought to enter cells via an endosomal pathway, is remarkably higher than those of other viruses which enter cells directly from the cell surface. The inhibition with HRP of influenza virus infection, which also uses an endosomal pathway, has not yet been reported, even though its hemagglutinin protein is the prototype class I fusion protein and its cell entry mechanism has been extensively studied. In contrast, HRP of avian leucosis sarcoma virus, which uses the endosomal pathway, was reported to inhibit the infection fairly efficiently (EC_{50} = 25 to 170 nM) (5, 23). The inhibition, however, was executed during the conformational rearrangement of the envelope protein that occurs on the cell surface following attachment to the receptor and facilitates the exposure of HRs but not later than the transport into the endosome, where the avian leucosis sarcoma virus genome enters the cytoplasm by its envelope and endosomal membrane fusion in a low-pH environment (19, 22, 23). These observations together with those of the present study and others (1, 18, 24, 45) suggest that the HRPs have very low or little inhibitory effect in the endosome. If the above assumption is correct and the HRPs were designed to be efficiently transferred into the endosome and to be stable in the environment, they may be new antiviral candidates against those viruses that take the endosomal entry pathway, such as influenza virus, Ebola virus, and SCoV. Thus, detailed molecular studies on SCoV and the sHRP will provide a good model for the development and evaluation of such endosome-philic antiviral peptide inhibitors.

Recent studies have reported that the low inhibitory effect of the SCoV sHRP compared to that of the MHV HRP could be attributed to the weaker interaction of the SCoV S HR1-HR2 complex versus that of MHV S (1, 2). However, SCoV infection was efficiently blocked by sHRP under certain conditions, as revealed in this study; the concentration of sHRPs needed to inhibit SCoV infection is even lower than that required for MHV inhibition (1, 2). The apparent difference between MHV and SCoV infection is the pathway used to enter cells; the former enters directly from the cell surface, whereas the latter takes an endosomal pathway. Both MHV and SCoV infections were efficiently blocked when these viruses utilized the cell surface pathway for entry. These observations suggest that the lower HRP inhibitory effect on SCoV could be due to different entry pathways between SCoV and MHV rather than the weaker interaction of the HRP and SCoV S. To further explore this possibility, studies are ongoing to determine the effect of MHV sHRPs on infection by MHV-2, which, like SCoV, utilizes an endosomal infection pathway (29).

We thank Miyuki Kawase for her excellent technical assistance and Shutoku Matsuyama for his valuable discussions.

This work was financially supported by grants from the Ministry of Education, Culture, Sports, Science and Technology.

REFERENCES

1. **Bosch, B. J., B. E. Martina, R. Van Der Zee, J. Lepault, B. J. Haijema, C. Versluis, A. J. Heck, R. De Groot, A. D. Osterhaus, and P. J. Rottier.** 2004. Severe acute respiratory syndrome coronavirus (SARS-CoV) infection inhibition using spike protein heptad repeat-derived peptides. Proc. Natl. Acad. Sci. USA **101**:8455–8460.
2. **Bosch, B. J., R. van der Zee, C. A. de Haan, and P. J. Rottier.** 2003. The coronavirus spike protein is a class I virus fusion protein: structural and functional characterization of the fusion core complex. J. Virol. **77**:8801–8811.
3. **Chan, W. E., C. K. Chuang, S. H. Yeh, M. S. Chang, and S. S. Chen.** 2006. Functional characterization of heptad repeat 1 and 2 mutants of the spike protein of severe acute respiratory syndrome coronavirus. J. Virol. **80**:3225–3237.
4. **Drosten, C., S. Gunther, W. Preiser, S. van der Werf, H. R. Brodt, S. Becker, H. Rabenau, M. Panning, L. Kolesnikova, R. A. Fouchier, A. Berger, A. M. Burguiere, J. Cinatl, M. Eickmann, N. Escriou, K. Grywna, S. Kramme, J. C. Manuguerra, S. Muller, V. Rickerts, M. Sturmer, S. Vieth, H. D. Klenk, A. D. Osterhaus, H. Schmitz, and H. W. Doerr.** 2003. Identification of a novel coronavirus in patients with severe acute respiratory syndrome. N. Engl. J. Med. **348**:1967–1976.
5. **Earp, L. J., S. E. Delos, R. C. Netter, P. Bates, and J. M. White.** 2003. The avian retrovirus avian sarcoma/leukosis virus subtype A reaches the lipid mixing stage of fusion at neutral pH. J. Virol. **67**:3058–3066.
6. **Follis, K. E., J. York, and J. H. Nunberg.** 2005. Serine-scanning mutagenesis studies of the C-terminal heptad repeats in the SARS coronavirus S glycoprotein highlight the important role of the short helical region. Virology **341**:122–129.
7. **Fouchier, R. A., T. Kuiken, M. Schutten, G. van Amerongen, G. J. van Doornum, B. G. van den Hoogen, M. Peiris, W. Lim, K. Stohr, and A. D. Osterhaus.** 2003. Aetiology: Koch's postulates fulfilled for SARS virus. Nature **423**:240.
8. **Huang, I. C., B. J. Bosch, F. Li, W. Li, K. H. Lee, S. Ghiran, N. Vasilieva, T. S. Dermody, S. C. Harrison, P. R. Dormitzer, M. Farzan, P. J. Rottier, and H. Choe.** 2006. SARS coronavirus, but not human coronavirus NL63, utilizes cathepsin L to infect ACE2-expressing cells. J. Biol. Chem. **281**:3198–3203.
9. **Inoue, Y., N. Tanaka, Y. Tanaka, S. Inoue, K. Morita, M. Zhuang, T. Hattori, and K. Sugamura.** 2007. Clathrin-dependent entry of severe acute respira-

tory syndrome coronavirus into target cells expressing ACE2 with the cytoplasmic tail deleted. J. Virol. 81:8722–8729.
10. Jahn, R., T. Lang, and T. C. Sudhof. 2003. Membrane fusion. Cell 112:519–533.
11. Jiang, S., K. Lin, N. Strick, and A. R. Neurath. 1993. HIV-1 inhibition by a peptide. Nature 365:113.
12. Joshi, S. B., R. E. Dutch, and R. A. Lamb. 1998. A core trimer of the paramyxovirus fusion protein: parallels to influenza virus hemagglutinin and HIV-1 gp41. Virology 248:20–34.
13. Kawabata, K., T. Hagio, and S. Matsuoka. 2002. The role of neutrophil elastase in acute lung injury. Eur. J. Pharmacol. 451:1–10.
14. Kilby, J. M., S. Hopkins, T. M. Venetta, B. DiMassimo, G. A. Cloud, J. Y. Lee, L. Alldredge, E. Hunter, D. Lambert, D. Bolognesi, T. Matthews, M. R. Johnson, M. A. Nowak, G. M. Shaw, and M. S. Saag. 1998. Potent suppression of HIV-1 replication in humans by T-20, a peptide inhibitor of gp41-mediated virus entry. Nat. Med. 4:1302–1307.
15. Ksiazek, T. G., D. Erdman, C. S. Goldsmith, S. R. Zaki, T. Peret, S. Emery, S. Tong, C. Urbani, J. A. Comer, W. Lim, P. E. Rollin, S. F. Dowell, A. E. Ling, C. D. Humphrey, W. J. Shieh, J. Guarner, C. D. Paddock, P. Rota, B. Fields, J. DeRisi, J. Y. Yang, N. Cox, J. M. Hughes, J. W. LeDuc, W. J. Bellini, and L. J. Anderson. 2003. A novel coronavirus associated with severe acute respiratory syndrome. N. Engl. J. Med. 348:1953–1966.
16. Lambert, D. M., S. Barney, A. L. Lambert, K. Guthrie, R. Medinas, D. E. Davis, T. Bucy, J. Erickson, G. Merutka, and S. R. Petteway, Jr. 1996. Peptides from conserved regions of paramyxovirus fusion (F) proteins are potent inhibitors of viral fusion. Proc. Natl. Acad. Sci. USA 93:2186–2191.
17. Li, F., M. Berardi, W. Li, M. Farzan, P. R. Dormitzer, and S. C. Harrison. 2006. Conformational states of the severe acute respiratory syndrome coronavirus spike protein ectodomain. J. Virol. 80:6794–6800.
18. Liu, S., G. Xiao, Y. Chen, Y. He, J. Niu, C. R. Escalante, H. Xiong, J. Farmar, A. K. Debnath, P. Tien, and S. Jiang. 2004. Interaction between heptad repeat 1 and 2 regions in spike protein of SARS-associated coronavirus: implications for virus fusogenic mechanism and identification of fusion inhibitors. Lancet 363:938–947.
19. Matsuyama, S., S. E. Delos, and J. M. White. 2004. Sequential roles of receptor binding and low pH in forming prehairpin and hairpin conformations of a retroviral envelope glycoprotein. J. Virol. 78:8201–8209.
20. Matsuyama, S., M. Ujike, S. Morikawa, M. Tashiro, and F. Taguchi. 2005. Protease-mediated enhancement of severe acute respiratory syndrome coronavirus infection. Proc. Natl. Acad. Sci. USA 102:12543–12547.
21. Medinas, R. J., D. M. Lambert, and W. A. Tompkins. 2002. C-Terminal gp40 peptide analogs inhibit feline immunodeficiency virus: cell fusion and virus spread. J. Virol. 76:9079–9086.
22. Melikyan, G. B., R. J. Barnard, R. M. Markosyan, J. A. Young, and F. S. Cohen. 2004. Low pH is required for avian sarcoma and leukosis virus Env-induced hemifusion and fusion pore formation but not for pore growth. J. Virol. 78:3753–3762.
23. Netter, R. C., S. M. Amberg, J. W. Balliet, M. J. Biscone, A. Vermeulen, L. J. Earp, J. M. White, and P. Bates. 2004. Heptad repeat 2-based peptides inhibit avian sarcoma and leukosis virus subgroup a infection and identify a fusion intermediate. J. Virol. 78:13430–13439.
24. Ni, L., J. Zhu, J. Zhang, M. Yan, G. F. Gao, and P. Tien. 2005. Design of recombinant protein-based SARS-CoV entry inhibitors targeting the heptad-repeat regions of the spike protein S2 domain. Biochem. Biophys. Res. Commun. 330:39–45.
25. Nicholls, J. M., L. L. Poon, K. C. Lee, W. F. Ng, S. T. Lai, C. Y. Leung, C. M. Chu, P. K. Hui, K. L. Mak, W. Lim, K. W. Yan, K. H. Chan, N. C. Tsang, Y. Guan, K. Y. Yuen, and J. S. Peiris. 2003. Lung pathology of fatal severe acute respiratory syndrome. Lancet 361:1773–1778.
26. Nie, Y., P. Wang, X. Shi, G. Wang, J. Chen, A. Zheng, W. Wang, Z. Wang, X. Qu, M. Luo, L. Tan, X. Song, X. Yin, J. Chen, M. Ding, and H. Deng. 2004. Highly infectious SARS-CoV pseudotyped virus reveals the cell tropism and its correlation with receptor expression. Biochem. Biophys. Res. Commun. 321:994–1000.
27. Otaka, A., M. Nakamura, D. Nameki, E. Kodama, S. Uchiyama, S. Nakamura, H. Nakano, H. Tamamura, Y. Kobayashi, M. Matsuoka, and N. Fujii. 2002. Remodeling of gp41-C34 peptide leads to highly effective inhibitors of the fusion of HIV-1 with target cells. Angew. Chem. Int. Ed. Engl. 41:2937–2940.
28. Petit, C. M., J. M. Melancon, V. N. Chouljenko, R. Colgrove, M. Farzan, D. M. Knipe, and K. G. Kousoulas. 2005. Genetic analysis of the SARS-coronavirus spike glycoprotein functional domains involved in cell-surface expression and cell-to-cell fusion. Virology 341:215–230.
29. Qiu, Z., S. T. Hingley, G. Simmons, C. Yu, J. Das Sarma, P. Bates, and S. R. Weiss. 2006. Endosomal proteolysis by cathepsins is necessary for murine coronavirus mouse hepatitis virus type 2 spike-mediated entry. J. Virol. 80:5768–5776.
30. Rapaport, D., M. Ovadia, and Y. Shai. 1995. A synthetic peptide corresponding to a conserved heptad repeat domain is a potent inhibitor of Sendai virus-cell fusion: an emerging similarity with functional domains of other viruses. EMBO J. 14:5524–5531.
31. Rota, P. A., M. S. Oberste, S. S. Monroe, W. A. Nix, R. Campagnoli, J. P. Icenogle, S. Penaranda, B. Bankamp, K. Maher, M. H. Chen, S. Tong, A. Tamin, L. Lowe, M. Frace, J. L. DeRisi, Q. Chen, D. Wang, D. D. Erdman, T. C. Peret, C. Burns, T. G. Ksiazek, P. E. Rollin, A. Sanchez, S. Liffick, B. Holloway, J. Limor, K. McCaustland, M. Olsen-Rasmussen, R. Fouchier, S. Gunther, A. D. Osterhaus, C. Drosten, M. A. Pallansch, L. J. Anderson, and W. J. Bellini. 2003. Characterization of a novel coronavirus associated with severe acute respiratory syndrome. Science 300:1394–1399.
32. Sagara, Y., Y. Inoue, H. Shiraki, A. Jinno, H. Hoshino, and Y. Maeda. 1996. Identification and mapping of functional domains on human T-cell lymphotropic virus type 1 envelope proteins by using synthetic peptides. J. Virol. 70:1564–1569.
33. Simmons, G., D. N. Gosalia, A. J. Rennekamp, J. D. Reeves, S. L. Diamond, and P. Bates. 2005. Inhibitors of cathepsin L prevent severe acute respiratory syndrome coronavirus entry. Proc. Natl. Acad. Sci. USA 102:11876–11881.
34. Simmons, G., J. D. Reeves, A. J. Rennekamp, S. M. Amberg, A. J. Piefer, and P. Bates. 2004. Characterization of severe acute respiratory syndrome-associated coronavirus (SARS-CoV) spike glycoprotein-mediated viral entry. Proc. Natl. Acad. Sci. USA 101:4240–4245.
35. Supekar, V. M., C. Bruckmann, P. Ingallinella, E. Bianchi, A. Pessi, and A. Carfi. 2004. Structure of a proteolytically resistant core from the severe acute respiratory syndrome coronavirus S2 fusion protein. Proc. Natl. Acad. Sci. USA 101:17958–17963.
36. Wang, E., X. Sun, Y. Qian, L. Zhao, P. Tien, and G. F. Gao. 2003. Both heptad repeats of human respiratory syncytial virus fusion protein are potent inhibitors of viral fusion. Biochem. Biophys. Res. Commun. 302:469–475.
37. Watanabe, S., A. Takada, T. Watanabe, H. Ito, H. Kida, and Y. Kawaoka. 2000. Functional importance of the coiled-coil of the Ebola virus glycoprotein. J. Virol. 74:10194–10201.
38. Wild, C., T. Oas, C. McDanal, D. Bolognesi, and T. Matthews. 1992. A synthetic peptide inhibitor of human immunodeficiency virus replication: correlation between solution structure and viral inhibition. Proc. Natl. Acad. Sci. USA 89:10537–10541.
39. Wild, C. T., D. C. Shugars, T. K. Greenwell, C. B. McDanal, and T. J. Matthews. 1994. Peptides corresponding to a predictive alpha-helical domain of human immunodeficiency virus type 1 gp41 are potent inhibitors of virus infection. Proc. Natl. Acad. Sci. USA 91:9770–9774.
40. Xu, Y., Z. Lou, Y. Liu, H. Pang, P. Tien, G. F. Gao, and Z. Rao. 2004. Crystal structure of severe acute respiratory syndrome coronavirus spike protein fusion core. J. Biol. Chem. 279:49414–49419.
41. Yang, Z. Y., Y. Huang, L. Ganesh, K. Leung, W. P. Kong, O. Schwartz, K. Subbarao, and G. J. Nabel. 2004. pH-dependent entry of severe acute respiratory syndrome coronavirus is mediated by the spike glycoprotein and enhanced by dendritic cell transfer through DC-SIGN. J. Virol. 78:5642–5650.
42. Yao, Q., and R. W. Compans. 1996. Peptides corresponding to the heptad repeat sequence of human parainfluenza virus fusion protein are potent inhibitors of virus infection. Virology 223:103–112.
43. Young, J. K., D. Li, M. C. Abramowitz, and T. G. Morrison. 1999. Interaction of peptides with sequences from the Newcastle disease virus fusion protein heptad repeat regions. J. Virol. 73:5945–5956.
44. Yu, M., E. Wang, Y. Liu, D. Cao, N. Jin, C. W. Zhang, M. Bartlam, Z. Rao, P. Tien, and G. F. Gao. 2002. Six-helix bundle assembly and characterization of heptad repeat regions from the F protein of Newcastle disease virus. J. Gen. Virol. 83:623–629.
45. Yuan, K., L. Yi, J. Chen, X. Qu, T. Qing, X. Rao, P. Jiang, J. Hu, Z. Xiong, Y. Nie, X. Shi, W. Wang, C. Ling, X. Yin, K. Fan, L. Lai, M. Ding, and H. Deng. 2004. Suppression of SARS-CoV entry by peptides corresponding to heptad regions on spike glycoprotein. Biochem. Biophys. Res. Commun. 319:746–752.

Design of a Novel HIV-1 Fusion Inhibitor That Displays a Minimal Interface for Binding Affinity

Shinya Oishi,*,† Saori Ito,† Hiroki Nishikawa,† Kentaro Watanabe,† Michinori Tanaka,† Hiroaki Ohno,† Kazuki Izumi,‡ Yasuko Sakagami,‡ Eiichi Kodama,‡ Masao Matsuoka,‡ and Nobutaka Fujii*,†

Graduate School of Pharmaceutical Sciences, Kyoto University, Sakyo-ku, Kyoto 606-8501, Japan, and Laboratory of Virus Immunology, Institute for Virus Research, Kyoto University, Sakyo-ku, Kyoto 606-8507, Japan

Received September 6, 2007

Abstract: Reported herein are the design, biological activities, and biophysical properties of a novel HIV-1 membrane fusion inhibitor. α-Helix-inducible X-EE-XX-KK motifs were applied to design an enfuvirtide analogue **2** that exhibited highly potent anti-HIV activity against wild-type HIV-1, enfuvirtide-resistant HIV-1 strains, and an HIV-2 strain in vitro. Indispensable residues for bioactivity of enfuvirtide, including the residues interacting with the N-terminal heptad repeat and the C-terminal hydrophobic residues, were identified.

The viral entry process of human immunodeficiency virus type 1 (HIV-1[a]) into target cells is mediated by envelope glycoprotein gp41. Formation of a fusogenic six-helical bundle structure consisting of a gp41 N-terminal heptad repeat (NHR) and C-terminal heptad repeat (CHR) promotes the fusion of viral and cellular membranes (Figure 1a).[1] Enfuvirtide **1** (T-20, DP178) is an approved anti-HIV peptide derived from the gp41 CHR.[2,3] This first drug that inhibits HIV-1 entry into the cell is utilized as an alternative anti-HIV agent for patients with drug resistance to reverse transcriptase and/or protease inhibitors. It is believed that peptide **1** interacts with the NHR of gp41 prehairpin structure[4] and associates with the cell or viral membrane through a C-terminal tryptophan-rich region,[5–7] but the exact action mechanism of **1** has not been clarified.[8,9]

Stabilization of bioactive conformations of peptides is a promising approach to enhance their biological potency and to understand the bioactive conformation. Several approaches to stabilize the α-helix structure of gp41 CHR have been reported including macrocyclization by covalent bond formation[10] or salt-bridge formation[11–13] between two adjacent residues and/or introduction of α-helix-inducible peptide sequences.[11] The analogue of another CHR peptide C34, in which the residues on the outer surface of the six-helical bundle were comprehensively replaced with glutamates (Glu) or lysines (Lys), retained highly potent anti-HIV activity.[12] This indicates that the substituted residues are not associated with an NHR coiled-coil as suggested by the crystal structure of the N36-C34 complex.[14] Our expectation was that the following three functional surfaces of **1** could be characterized by extending this molecular design (Figure 1b): (1) minimal interface residues for affinity with NHR; (2) solvent-accessible sites to be utilized for α-helix inducible salt bridges; (3) another functional region outside the α-helix structure. Accordingly, efforts herein were undertaken to design novel amphiphilic enfuvirtide derivatives bearing α-helix-inducible motifs.

A schematic wheel of the potential α-helix structure of peptide **1** is depicted in Figure 1c. To introduce salt bridges between *i* and *i* + 4 residues on the basis of the previous C34 modification,[12] Glu and Lys were arranged at b/c and f/g positions, respectively, so that four consecutive X-EE-XX-KK motifs appeared in the designed peptide **2** (designated T-20EK, Figure 2). All peptides were prepared by standard Fmoc-based peptide synthesis protocol. After final deprotection and cleavage from the resins using a TFA/thioanisole/*m*-cresol/ethanedithiol/H_2O (80:5:5:5:5) cocktail, the crude peptides were purified by reverse-phase HPLC to yield the expected peptides, which were characterized by mass spectrometry. Anti-HIV activity of the peptides against laboratory HIV-1 NL4-3 strain (wild-type) was evaluated by MAGI assay (Table 1). Peptide **2** exhibited 8-fold greater anti-HIV activity compared with the parent peptide **1** [peptide **1**, EC_{50} = 15 ± 3.9 nM; peptide **2**, EC_{50} = 1.8 ± 0.4 nM].[15] The circular dichroism (CD) spectrum of **2** in phosphate buffered saline (pH 7.4) had negative minima at 208 and 222 nm, indicating the presence of an α-helical conformation, while that of **1** suggested a random-coil conformation (Figure 3a). The significant increase in anti-HIV activity of **2** could be rationalized by the preordered stable α-helical structure upstream of L158.[16]

Systematic substitutions of the amino acids at the b, c, f, and g positions with Glu or Lys were extended (Figure 2). Peptide **3**, in which L130 and N160 were substituted with Lys and Glu, respectively, showed anti-HIV activity similar to that of peptide **2** (peptide **3**, EC_{50} = 2.8 ± 0.6 nM). This is consistent with the fact that potent T-1249 also contains these two substitutions.[17] Further replacement toward the N-terminal f position (S129) was again permissive of the high anti-HIV activity (peptide **4**, EC_{50} = 2.5 ± 0.6 nM). On the other hand, replacement of W161 with Glu resulted in a significant decrease of anti-HIV activity as observed in peptides **5** and **6** (EC_{50} = 185 and 111 nM, respectively), indicating that W161 may be located outside the amphiphilic α-helical region. This result correlates with the reduced entry ability of W161F mutant virus.[18] Alanine substitution of W161 also supports the relevance of this residue in virus infectivity and in the inhibitory activity of **1**. Although peptide **7**, carrying a W155A substitution, expressed anti-HIV activity similar to that of peptide **2** (peptide **7**, EC_{50} = 5.8 ± 1.0 nM), W159A, W161A, and F162A substitutions showed reduced bioactivity (peptides **8**, **9**, and **10**, EC_{50} = 49, 24, and 27 nM, respectively). The observed similar CD spectra among peptides **2** and **7–10** demonstrated that alanine substitution had no effect on the stabilized secondary structure of the α-helix (Figure 3b). That is, the hydrophobic indole and phenyl groups of these peptides may contribute to their direct interaction with virus components such as gp41 NHR or the virus membrane.[19]

The comparative binding affinity of peptides **1** and **2** with the gp41 NHR sequence was investigated by pull-down assay using synthetic His-tagged CHR peptides and recombinant MBP-fused NHR protein (Figure 4a). Peptide **2** showed higher affinity with NHR compared with **1**. In contrast, only weak binding was observed in the same experiment using all-D-T-20EK D-**2**, which consists of all D-amino acids, indicating that

* To whom correspondence should be addressed. Phone: +81-75-753-4551. Fax: +81-75-753-4570. E-mail: for S.O., soishi@pharm.kyoto-u.ac.jp; for N.F., nfujii@pharm.kyoto-u.ac.jp.

† Graduate School of Pharmaceutical Sciences.

‡ Institute for Virus Research.

[a] Abbreviations: HIV-1, human immunodeficiency virus type 1; NHR, N-terminal heptad repeat; CHR, C-terminal heptad repeat.

10.1021/jm701109d CCC: $40.75
Published on Web 01/16/2008

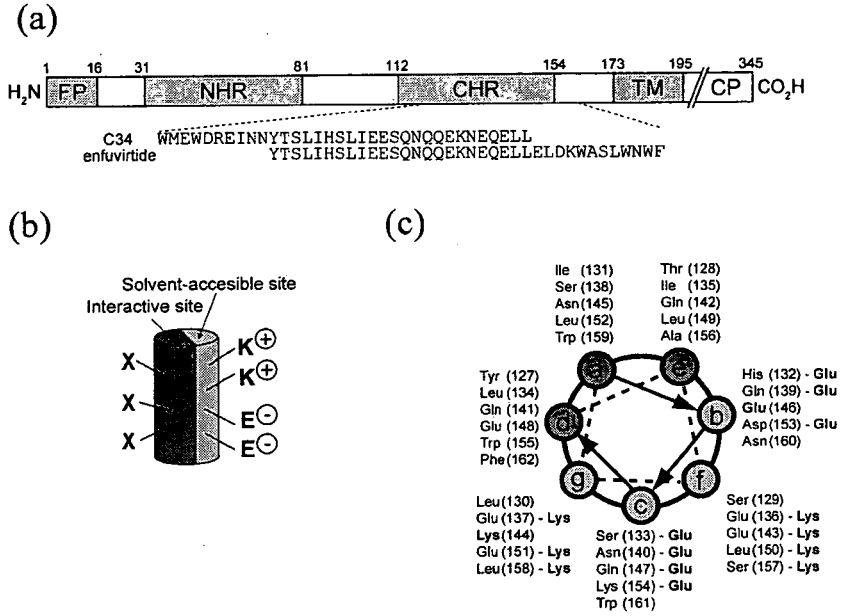

Figure 1. Design of enfuvirtide analogues: (a) schematic representation of HIV-1 gp41 (FP, fusion peptide; NHR, N-terminal heptad repeat; CHR, C-terminal heptad repeat; TM, transmembrane domain); (b) estimated preordered α-helix structure of CHR peptide by potential salt-bridge formation; (c) helical-wheel representation of peptides **1** and **2**. For peptide **2**, Glu residues are in b and c positions and Lys residues in f and g positions. Residues are numbered starting at the first amino acid of the NL4-3 gp41.

```
Ac-YTSLIHSLIEESQNQQEKNEQELLELDKWASLWNWF-CONH2  1 (enfuvirtide)
Ac------EE--KK-EE--K---E--KK-EE--KK-----CONH2  2
Ac----K-EE--KK-EE--K---E--KK-EE--KK-E---CONH2  3
Ac---KK-EE--KK-EE--K---E--KK-EE--KK-E---CONH2  4
Ac----K-EE--KK-EE--K---E--KK-EE--KK-EE--CONH2  5
Ac---KK-EE--KK-EE--K---E--KK-EE--KK-EE--CONH2  6
Ac------EE--KK-EE--K---E--KK-EEA-KK-----CONH2  7
Ac------EE--KK-EE--K---E--KK-EE--KKA----CONH2  8
Ac------EE--KK-EE--K---E--KK-EE--KK--A--CONH2  9
Ac------EE--KK-EE--K---E--KK-EE--KK---A-CONH2  10
  Ac-LDAN-TK-L--A-I-----MY--QK-NQ-DIFS----CONH2  11
Ac-WQEWEQK-TA-L-QA-I------Y--QK--------E---CONH2  T-1249
```

Figure 2. Peptide sequences of enfuvirtide, enfuvirtide analogues, and T-1249.

Table 1. Anti-HIV Activity of Synthetic Enfuvirtide Analogues

peptide	EC_{50} (nM)[a]	peptide	EC_{50} (nM)[a]
1 (enfuvirtide)	15 ± 3.9	**7**	5.8 ± 1.0
2[b]	1.8 ± 0.4	**8**	49 ± 8.6
3	2.8 ± 0.6	**9**	24 ± 3.8
4	2.5 ± 0.6	**10**	27 ± 6.8
5	185 ± 17	C34	4.5 ± 0.5
6	111 ± 25		

[a] EC_{50} was determined as the concentration that blocked HIV-1 replication by 50% in MAGI assay. [b] The enantiomer of peptide **2** (D-**2**) did not show anti-HIV activity at 10 μM.

the binding between **2** and NHR is specific. In addition, peptide **2** inhibited the interaction between **1** and NHR in lower concentration in the inhibition experiment (Figure 4b).[20]

We next evaluated the anti-HIV activity of peptide **2** against enfuvirtide-resistant variants HIV-1_{V38A} and HIV-1_{N43D}, which were mainly isolated from patients resistant to enfuvirtide (Table 2).[21] Because of the deficient replication of these variants,[22] an additional D36G mutation was experimentally added to these variants and to the wild-type virus. The D36G mutation is not involved in enfuvirtide resistance, but it did improve the sensitivity against **1** [EC_{50}(HIV-1_{D36G}) = 2.3 nM] compared with wild-type HIV-1. As reported previously,[21] V38A and N43D mutations significantly reduced the potency of **1** [EC_{50} (HIV-1_{V38A}) = 22 nM; EC_{50}(HIV-1_{N43D}) = 46 nM]. On the other hand, peptide **2** retained similar anti-HIV activity against N43D and slightly less potent activity toward V38A variants [EC_{50}(HIV-1_{V38A}) = 3.3 nM; EC_{50}(HIV-1_{N43D}) = 1.7 nM]. It is of interest that the anti-HIV activity was restored by induction of a bioactive α-helix structure using X-EE-XX-KK motifs on a CHR peptide. This implies that the stable α-helical structure of **2** can overcome the reduced affinity derived from the mismatched interaction between mutated NHR sequences and peptide **1**.

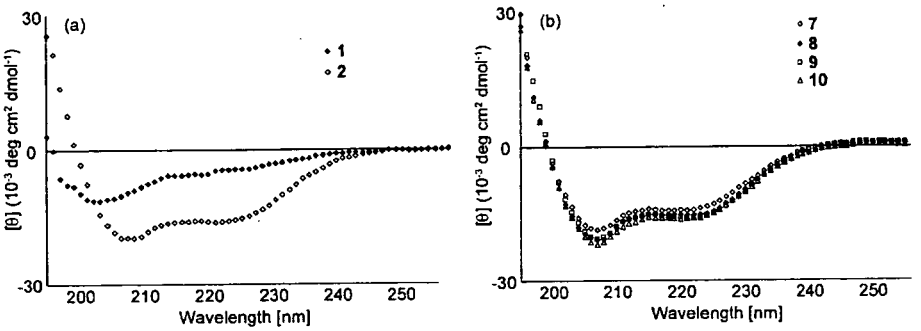

Figure 3. Circular dichroism spectra of (a) peptides **1** and **2** and (b) Ala-substituted peptides **7–10**.

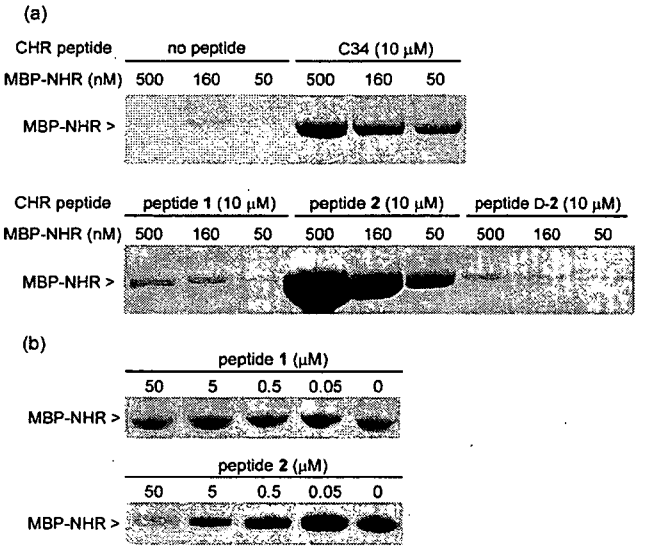

Figure 4. Interaction of His-tagged CHR peptides with MBP-NHR protein by pull-down assay and SDS−PAGE: (a) NHR protein binding with several His-tagged CHR peptides; (b) inhibition of interaction between His-tagged enfuvirtide and NHR protein by nontagged peptides **1** and **2**.

Table 2. Anti-HIV Activity of Peptides 1 and 2 against Enfuvirtide-Resistant Variant and HIV-2 Strains

	EC_{50} (nM)[a]	
strains	peptide **1**	peptide **2**
HIV-1		
NL4–3	15 ± 3.9	1.8 ± 0.4
D36G	2.3 ± 0.5	0.9 ± 0.2
D36G V38A	22 ± 7.6	3.3 ± 1.0
D36G N43D	46 ± 9.6	1.7 ± 0.3
HIV-2		
EHO[b]	37 ± 10	1.5 ± 0.5

[a] EC_{50} was determined as the concentration that blocked HIV-1 replication by 50% in MAGI assay. [b] The antiviral activity (EC_{50}) of peptide **11** against EHO strain was 2.1 ± 0.7 nM.

Interestingly, peptide **2** showed potent antiviral activity even against an HIV-2 EHO strain [EC_{50} = 1.5 nM], which is as potent as peptide **11** having a congenerous sequence derived from the EHO strain [EC_{50} = 2.1 nM].[23] This is in contrast to the previous report on the reduced activity of **1** against the EHO strain [EC_{50} = 37 nM].[24] The potent bioactivity of **2** can be rationalized by the minimal difference of the interface residues between HIV-1 and -2 and the stabilized α-helix structure. Among 19 different residues between the sequences of NL4-3 and EHO strains, 13 residues are located at the solvent accessible sites (b, c, f, and g positions). Although the other six residues are possibly involved in the direct interaction, the potential reduced interactions derived from the mismatch could be recovered by introduction of X-EE-XX-KK motifs.

In conclusion, remodeling of **1** to yield the preordered α-helical structure of **2** led to improved affinity with NHR and increased antiviral activity even against enfuvirtide-resistant HIV-1 and HIV-2 strains. This approach also helped to clarify the potential minimal interface of **1** with viral gp41. Peptide **2** could be a useful chemical tool to understand the membrane fusion process of HIV-1 and the detailed action mechanism of enfuvirtide.

Acknowledgment. This work was supported by a Grant-in-Aid for Scientific Research from the Ministry of Education, Culture, Sports, Science, and Technology of Japan, Health and Labour Sciences Research Grants (Research on HIV/AIDS), the 21st Century COE Program's "Knowledge Information Infrastructure for Genome Science", and the Japan Science and Technology Agency. H.N. is grateful for the JSPS Research Fellowships for Young Scientists. Appreciation is expressed to Dr. Masaru Hoshino (Kyoto University) for helpful discussions and to Mr. Maxwell Reback (Kyoto University) for reading the manuscript.

Supporting Information Available: Experimental details for peptide preparation, CD spectra measurements, and bioassays and MS and HPLC data. This material is available free of charge via the Internet at http://pubs.acs.org.

References

(1) Lu, M.; Blacklow, S. C.; Kim, P. S. A trimeric structural domain of the HIV-1 transmembrane glycoprotein. *Nat. Struct. Biol.* **1995**, *2*, 1075–1082.
(2) Wild, C. T.; Shugars, D. C.; Greenwell, T. K.; McDanal, C. B.; Matthews, T. J. Peptides corresponding to a predictive alpha-helical domain of human immunodeficiency virus type 1 gp41 are potent inhibitors of virus infection. *Proc. Natl. Acad. Sci. U.S.A.* **1994**, *91*, 9770–9774.
(3) Matthews, T.; Salgo, M.; Greenberg, M.; Chung, J.; DeMasi, R.; Bolognesi, D. Enfuvirtide: the first therapy to inhibit the entry of HIV-1 into host CD4 lymphocytes. *Nat. Rev. Drug. Discovery* **2004**, *3*, 215–225.
(4) Lawless, M. K.; Barney, S.; Guthrie, K. I.; Bucy, T. B.; Petteway, S. R., Jr.; Merutka, G. HIV-1 membrane fusion mechanism: structural studies of the interactions between biologically-active peptides from gp41. *Biochemistry* **1996**, *35*, 13697–13708.
(5) Kliger, Y.; Gallo, S. A.; Peisajovich, S. G.; Munoz-Barroso, I.; Avkin, S.; Blumenthal, R.; Shai, Y. Mode of action of an antiviral peptide from HIV-1. Inhibition at a post-lipid mixing stage. *J. Biol. Chem.* **2001**, *276*, 1391–1397.
(6) Cardoso, R. M.; Zwick, M. B.; Stanfield, R. L.; Kunert, R.; Binley, J. M.; Katinger, H.; Burton, D. R.; Wilson, I. A. Broadly neutralizing anti-HIV antibody 4E10 recognizes a helical conformation of a highly conserved fusion-associated motif in gp41. *Immunity* **2005**, *22*, 163–173.
(7) Wexler-Cohen, Y.; Johnson, B. T.; Puri, A.; Blumenthal, R.; Shai, Y. Structurally altered peptides reveal an important role for N-terminal heptad repeat binding and stability in the inhibitory action of HIV-1 peptide DP178. *J. Biol. Chem.* **2006**, *281*, 9005–9010.
(8) Liu, S.; Lu, H.; Niu, J.; Xu, Y.; Wu, S.; Jiang, S. Different from the HIV fusion inhibitor C34, the anti-HIV drug Fuzeon (T-20) inhibits HIV-1 entry by targeting multiple sites in gp41 and gp120. *J. Biol. Chem.* **2005**, *280*, 11259–11273.
(9) Liu, S.; Jing, W.; Cheung, B.; Lu, H.; Sun, J.; Yan, X.; Niu, J.; Farmar, J.; Wu, S.; Jiang, S. HIV gp41 C-terminal heptad repeat contains multifunctional domains. Relation to mechanisms of action of anti-HIV peptides. *J. Biol. Chem.* **2007**, *282*, 9612–9620.
(10) Judice, J. K.; Tom, J. Y.; Huang, W.; Wrin, T.; Vennari, J.; Petropoulos, C. J.; McDowell, R. S. Inhibition of HIV type 1 infectivity by constrained α-helical peptides: implications for the viral fusion mechanism. *Proc. Natl. Acad. Sci. U.S.A.* **1997**, *94*, 13426–13430.
(11) Joyce, J. G.; Hurni, W. M.; Bogusky, M. J.; Garsky, V. M.; Liang, X.; Citron, M. P.; Danzeisen, R. C.; Miller, M. D.; Shiver, J. W.; Keller, P. M. Enhancement of α-helicity in the HIV-1 inhibitory peptide DP178 leads to an increased affinity for human monoclonal antibody 2F5 but does not elicit neutralizing responses in vitro. *J. Biol. Chem.* **2002**, *277*, 45811–45820.
(12) Otaka, A.; Nakamura, M.; Nameki, D.; Kodama, E.; Uchiyama, S.; Nakamura, S.; Nakano, H.; Tamamura, H.; Kobayashi, Y.; Matsuoka, M.; Fujii, N. Remodeling of gp41-C34 peptide leads to highly effective inhibitors of the fusion of HIV-1 with target cells. *Angew. Chem., Int. Ed.* **2002**, *41*, 2937–2940.
(13) Dwyer, J. J.; Wilson, K. L.; Davison, D. K.; Freel, S. A.; Seedorff, J. E.; Wring, S. A.; Tvermoes, N. A.; Matthews, T. J.; Greenberg, M. L.; Delmedico, M. K. Design of helical, oligomeric HIV-1 fusion inhibitor peptides with potent activity against enfuvirtide-resistant virus. *Proc. Natl. Acad. Sci. U.S.A.* **2007**, *104*, 12772–12777.
(14) Chan, D. C.; Fass, D.; Berger, J. M.; Kim, P. S. Core structure of gp41 from the HIV envelope glycoprotein. *Cell* **1997**, *89*, 263–273.
(15) Cytotoxicity of peptide **2** was not observed even at 10 μM.
(16) Additional effects on increasing the anti-HIV activity such as formation of intra- and intermolecular salt bridges are also possible.
(17) Eron, J. J.; Gulick, R. M.; Bartlett, J. A.; Merigan, T.; Arduino, R.; Kilby, J. M.; Yangco, B.; Diers, A.; Drobnes, C.; DeMasi, R.;

Greenberg, M.; Melby, T.; Raskino, C.; Rusnak, P.; Zhang, Y.; Spence, R.; Miralles, G. D. Short-term safety and antiretroviral activity of T-1249, a second-generation fusion inhibitor of HIV. *J. Infect. Dis.* **2004**, *189*, 1075–1083.

(18) Salzwedel, K.; West, J. T.; Hunter, E. A conserved tryptophan-rich motif in the membrane-proximal region of the human immunodeficiency virus type 1 gp41 ectodomain is important for Env-mediated fusion and virus infectivity. *J. Virol.* **1999**, *73*, 2469–2480.

(19) Wexler-Cohen, Y.; Johnson, B. T.; Puri, A.; Blumenthal, R.; Shai, Y. Structurally altered peptides reveal an important role for N-terminal heptad repeat binding and stability in the inhibitory action of HIV-1 peptide DP178. *J. Biol. Chem.* **2006**, *281*, 9005–9010.

(20) Since a large excess of CHR peptides to NHR protein was utilized for the pull-down assay, the inhibitory concentration in this experiment was less than that observed in the MAGI assay. It is conceivable that the anti-HIV activity in the MAGI assay might be observed with less fully occupied one or two CHR peptides bound per NHR trimer.

(21) Cabrera, C.; Marfil, S.; Garcia, E.; Martinez-Picado, J.; Bonjoch, A.; Bofill, M.; Moreno, S.; Ribera, E.; Domingo, P.; Clotet, B.; Ruiz, L. Genetic evolution of gp41 reveals a highly exclusive relationship between codons 36, 38 and 43 in gp41 under long-term enfuvirtide-containing salvage regimen. *AIDS* **2006**, *20*, 2075–2080.

(22) Mink, M.; Mosier, S. M.; Janumpalli, S.; Davison, D.; Jin, L.; Melby, T.; Sista, P.; Erickson, J.; Lambert, D.; Stanfield-Oakley, S. A.; Salgo, M.; Cammack, N.; Matthews, T.; Greenberg, M. L. Impact of human immunodeficiency virus type 1 gp41 amino acid substitutions selected during enfuvirtide treatment on gp41 binding and antiviral potency of enfuvirtide in vitro. *J. Virol.* **2005**, *79*, 12447–12454.

(23) Gustchina, E.; Hummer, G.; Bewley, C. A.; Clore, G. M. Differential inhibition of HIV-1 and SIV envelope-mediated cell fusion by C34 peptides derived from the C-terminal heptad repeat of gp41 from diverse strains of HIV-1, HIV-2, and SIV. *J. Med. Chem.* **2005**, *48*, 3036–3044.

(24) Witvrouw, M.; Pannecouque, C.; Switzer, W. M.; Folks, T. M.; De Clercq, E.; Heneine, W. Susceptibility of HIV-2, SIV and SHIV to various anti-HIV-1 compounds: implications for treatment and post-texposure prophylaxis. *Antiviral Ther.* **2004**, *9*, 57–65.

JM701109D

Facile synthesis of 3-(aminomethyl)isoquinolines by copper-catalysed domino four-component coupling and cyclisation†

Yusuke Ohta, Shinya Oishi, Nobutaka Fujii* and Hiroaki Ohno*

Received (in Cambridge, UK) 26th November 2007, Accepted 12th December 2007
First published as an Advance Article on the web 4th January 2008
DOI: 10.1039/b718201e

Copper(I)-catalysed domino four-component coupling–cyclisation using 2-ethynylbenzaldehydes, paraformaldehyde, secondary amine, and *t*-BuNH$_2$ in DMF leads to direct and efficient formation of 3-(aminomethyl)isoquinolines in good to high yields.

The isoquinoline scaffold can be found in a wide variety of biologically active natural and synthetic compounds.[1] Particularly, isoquinolines having an additional nitrogen atom tethered by one carbon at the 3-position, including such isoquinoline alkaloids as quinocarcin[2] and ecteinascidin 597 and 583,[3] and 3-(2-pyridinyl)isoquinolines,[4] constitute an important class of compounds with important biological activities. With a continuing interest in the development of environmentally-benign synthesis as well as multi-component reactions in modern synthetic chemistry,[5] we planned a novel diversity-oriented synthetic methodology for the construction of these molecules by the use of a domino multi-component coupling–cyclisation reaction.

Recently, we have reported an efficient construction of 2-(aminomethyl)indoles by a copper-catalysed three-component coupling–cyclisation reaction.[6] This reaction proceeds through Mannich-type coupling followed by indole formation. On the basis of our indole synthesis, we expected that a four-component coupling reaction of 2-ethynylbenzaldehydes **1**, aldehyde **2**, secondary amine **3**, and an appropriate N-1 synthon **4**, followed by cyclisation of the alkyne intermediate **5**, having a nitrogen atom in proximity to the triple bond,[7,8] would provide a direct route to 3-(aminomethyl)isoquinolines **6** without wasting any salts (Scheme 1). Herein, we describe a copper-catalysed domino four-component coupling–cyclisation reaction for diversity-oriented synthesis of 3-(aminomethyl)isoquinolines. To the best of our knowledge, this is the first example of a four-component synthesis of an isoquinoline scaffold.[9]

In the initial investigation, we examined the effect of the N-1 synthon on the copper-catalysed four-component synthesis of 3-(aminomethyl)isoquinoline using 2-ethynylbenzaldehyde **1a** as a model substrate, paraformaldehyde **2** and diisopropylamine **3a** (Table 1). Since two nucleophilic reagents coexist with two aldehydes in the reaction system, progress of the

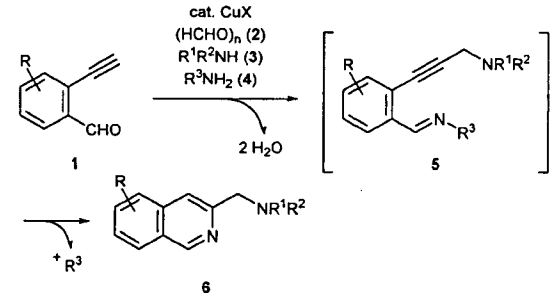

Scheme 1 Construction of 3-(aminomethyl)isoquinolines by copper-catalysed four-component coupling–cyclisation.

nucleophilic reactions in the desired order might be hampered on one-portion reaction.[10] Accordingly, after the copper-catalysed three component reaction of **1a**, **2**, and **3a** in DMF was complete, being monitored by TLC, the N-1 synthon was added. Whereas ammonium nitrate **4a**, perchlorate **4b**, hydroxide **4c**, formate **4d**, chloride **4e**, and sulfate **4f** were ineffective (entries 1–6), the use of acetate **4g** and hydrogen carbonate **4h** gave, as expected, the desired isoquinoline **6a** in moderate yields (42–53%, entries 7 and 8).[11] More promising results were obtained with primary amines having a readily cleavable alkyl group such as 2,4,6-trimethoxybenzylamine hydrochloride **4i** and *tert*-butylamine **4j**,[7] leading to high yields of **6a**

Table 1 Optimisation of the N-1 synthon **4**[a]

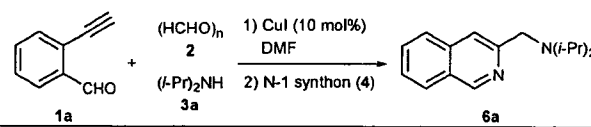

Entry	N-1 synthon	Yield (%)[b]
1	NH_4NO_3 (**4a**)	Decomp.
2	NH_4ClO_4 (**4b**)	Decomp.
3	28% NH_4OH (**4c**)	Trace
4	$NH_4(HCO_2)$ (**4d**)	Trace
5	NH_4Cl (**4e**)	Trace
6	$(NH_4)_2SO_4$ (**4f**)	Trace
7	NH_4OAc (**4g**)	42
8	NH_4HCO_3 (**4h**)	53
9	2,4,6-$(MeO)_3C_6H_2CH_2NH_2 \cdot HCl$ (**4i**)	82
10	*t*-$BuNH_2$ (**4j**)	83

[a] After a mixture of 2-ethynylbenzaldehyde **1a**, paraformaldehyde **2** (2 equiv.), amine **3a** (2 equiv.) and CuI (10 mol%) in DMF was stirred at room temperature for 1 h, and N-1 synthon **4** (6 equiv.) was added. The resulting mixture was stirred for 5 h at room temperature and for an additional 45 min at 140 °C. [b] Isolated yield.

Graduate School of Pharmaceutical Sciences, Kyoto University, Sakyo-ku, Kyoto 606-8501, Japan. E-mail: nfujii@pharm.kyoto-u.ac.jp. E-mail: hohno@pharm.kyoto-u.ac.jp
† Electronic supplementary information (ESI) available: Experimental details and NMR spectra. See DOI: 10.1039/b718201e

Table 2 Synthesis of 3-(aminomethyl)isoquinolines[a]

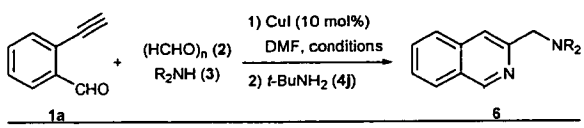

Entry	Amine	Conditions[b]	Product	Yield (%)[d]
1	i-Pr$_2$NH (3a)	rt, 1 h	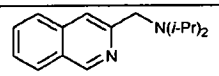 6a	83
2	Bn$_2$NH (3b)	100 °C, 1 h	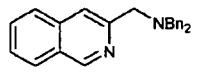 6b	0
3	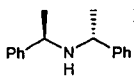 3c	100 °C, 1 h	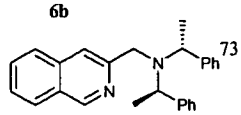 6c	73
4	(allyl)$_2$NH (3d)	rt, 1 h[c]	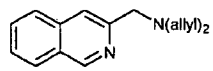 6d	60
5	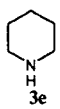 3e	rt, 1 h[c]	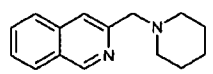 6e	88
6	 3f	rt, 1 h[c]	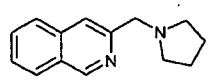 6f	79

[a] After the three-component reaction of **1a**, **2** (2 equiv.), and **3** (2 equiv.) in the presence of CuI (10 mol%) in DMF was completed on TLC, t-BuNH$_2$ (**4j**, 6 equiv.) was added and the reaction mixture was stirred for 5 h at room temperature and for an additional 45 min at 140 °C. [b] Conditions for the three-component coupling. [c] Before **1a** was added, a mixture of **2**, **3** and CuI in DMF was stirred for 30 min at room temperature. [d] Isolated yield.

(entries 9 and 10).[12] Taking the atom economy of the reaction into consideration, we regarded **4j** as the most potent N-1 synthon.

Next, various secondary amines were employed to determine the scope of this reaction (Table 2). Although dibenzylamine **3b** showed lower reactivity toward Mannich-type coupling with **1a** and **2**, leading to recovery of the unchanged starting material (entry 2),[13] the reaction with more bulky bis(1-phenylethyl)amine **3c** led to successful conversion into the corresponding isoquinoline **6c** (73%, entry 3). Unfortunately, the initial Mannich type reaction with highly nucleophilic diallylamine, piperidine, or pyrrolidine was unsuccessful, producing a complex mixture, presumably due to the simultaneous presence of two aldehydes (2-ethynylbenzaldehyde **1a** and paraformaldehyde **2**) and a reactive amine. Extensive optimisation of the reaction conditions brought about addition of 2-ethynylaldehyde **1a** after the formation of iminium ions between secondary amines **3d–f** and paraformaldehyde **2**. As a result, the corresponding 3-(aminomethyl)isoquinolines **6d–f** were obtained in moderate to high yields (entries 4–6).

The copper-catalysed domino four-component syntheses of 3-(aminomethyl)isoquinolines with some substituted 2-ethynylbenzaldehydes were next investigated (Table 3). The use of 2-ethynyl-4-fluorobenzaldehyde **1b** in the presence of CuI (10 mol%) gave the desired 3-(aminomethyl)-6-fluoroisoquinoline derivative **7** in high yield (83%, entry 1). Benzaldehyde **1c**, which has a fluorine atom at the *meta*-position to the formyl group, afforded the corresponding isoquinoline **8** (79%, entry 2). Also, in the cases of 2-ethynylbenzaldehydes containing an electron-donating group such as a methyl or a methoxy group at the *para*- or *meta*-position to the formyl group (**1d** and **1e**, respectively), the copper-catalysed four-component isoquinoline formation proceeded smoothly (87 and 84% yield, respectively, entries 3 and 4). Thus, this isoquinoline formation was proven to be widely applicable to 2-ethynylbenzaldehydes having an electron-withdrawing and -donating group.

Table 3 Reactions with substituted 2-ethynylbenzaldehydes[a]

Entry	Substrate	Product	Yield (%)[b]
1	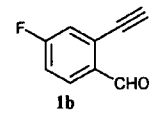 1b	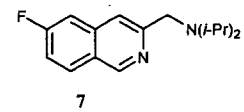 7	83
2	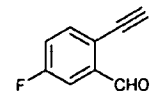 1c	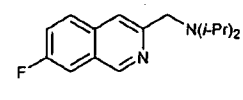 8	79
3	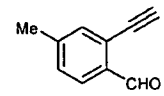 1d	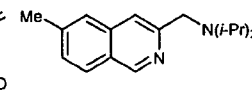 9	87
4	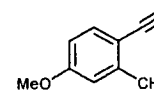 1e	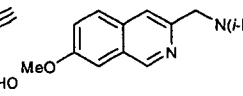 10	84

[a] After the three-component reaction of **1**, **2** (2 equiv.), and **3a** (2 equiv.) in the presence of CuI (10 mol%) in DMF was completed on TLC, t-BuNH$_2$ (**4j**, 6 equiv.) was added and the reaction mixture was stirred for 5 h at room temperature and for an additional 45 min at 140 °C. [b] Isolated yield.

In conclusion, we have developed a novel copper-catalysed domino four-component coupling–cyclisation reaction for the synthesis of 3-(aminomethyl)isoquinolines, which form one carbon–carbon and three carbon–nitrogen bonds. This methodology could be applied to the construction of a highly potent isoquinoline library in terms of diversity and biological activity.

Notes and references

1 For recent reviews, see: (*a*) J. D. Scott and R. M. Williams, *Chem. Rev.*, 2002, **102**, 1669–1730; (*b*) M. Chrzanowska and M. D. Rozwadowska, *Chem. Rev.*, 2004, **104**, 3341–3370. For recent examples, see: (*c*) A. Bermejo, I. Andreu, F. Suvire, S. Leonce, D. H. Caignard, P. Renard, A. Pierré, R. D. Enriz, E. Cortes and N. Cabedo, *J. Med. Chem.*, 2002, **45**, 5058–5068; (*d*) A. Morrel, S. Antony, G. Kohlhagen, Y. Pommier and M. Cushman, *J. Med. Chem.*, 2006, **49**, 7740–7753; (*e*) G. Bringmann, M. Dreyer, J. H. Faber, P. W. Dalsgaard, D. Stærk, J. W. Jaroszewski,

H. Ndangalasi, F. Mbago, R. Brun and S. B. Christensen, *J. Nat. Prod.*, 2004, **67**, 743–748; (*f*) A. Graulich, F. Mercier, J. Scuvée-Moreau, V. Seutin and J. F. Liégeois, *Bioorg. Med. Chem.*, 2005, **13**, 1201–1209; (*g*) Y. H. Chen, Y. H. Zhang, H. J. Zhang, D. Z. Liu, M. Gu, J. Y. Li, F. Wu, X. Z. Zhu, J. Li and F. J. Nan, *J. Med. Chem.*, 2006, **49**, 1613–1623; (*h*) A. Morrel, S. Antony, G. Kohlhagen, Y. Pommier and M. Cushman, *J. Med. Chem.*, 2006, **49**, 7740–7753; (*i*) G. Bringmann, J. Mutanyatta-Comar, M. Greb, S. Rüdenauer, T. F. Noll and A. Irmer, *Tetrahedron*, 2007, **63**, 1755–1761.

2 For the isolation, see: (*a*) F. Tomita, K. Takahashi and K. Shimizu, *J. Antibiot.*, 1983, 463–467; (*b*) K. Takahashi and F. Tomita, *J. Antibiot.*, 1983, 468–470. For the total synthesis, see: (*c*) T. Fukuyama and J. J. Nunes, *J. Am. Chem. Soc.*, 1988, **110**, 5196–5198; (*d*) S. Kwon and A. G. Myers, *J. Am. Chem. Soc.*, 2005, **127**, 16796–16797.

3 For the isolation, see: (*a*) R. Sakai, E. A. Jares-Erijman, I. Manzanares, M. V. S. Elipe and K. L. Rinehart, *J. Am. Chem. Soc.*, 1996, **118**, 9017–9023. For the total synthesis, see: (*b*) J. Chen, X. Chen, M. Willot and J. Zhu, *Angew. Chem., Int. Ed.*, 2006, **45**, 8028–8032.

4 (*a*) M. A. H. de Zwart, H. van der Goot and H. Timmerman, *J. Med. Chem.*, 1989, **32**, 487–493; (*b*) J. E. van Muijlwijk-Koezen, H. Timmerman, R. Link, H. van der Goot and A. P. IJzerman, *J. Med. Chem.*, 1998, **41**, 3987–3993; (*c*) J. E. van Muijlwijk-Koezen, H. Timmerman, R. Link, H. van der Goot and A. P. IJzerman, *J. Med. Chem.*, 1998, **41**, 3994–4000.

5 For recent notable reviews, see: (*a*) B. M. Trost, *Acc. Chem. Res.*, 2002, **35**, 695–705; (*b*) K. C. Nicolaou, T. Montagnon and S. A. Snyder, *Chem. Commun.*, 2003, 551–564.

6 H. Ohno, Y. Ohta, S. Oishi and N. Fujii, *Angew. Chem., Int. Ed.*, 2007, **46**, 2295–2298.

7 For copper-catalysed isoquinoline formation through *N-tert*-butyl-2-(1-alkynyl)benzaldimine derivatives, see: (*a*) K. R. Roesh and R. C. Larock, *J. Org. Chem.*, 1998, **63**, 5306–5307; (*b*) K. R. Roesch and R. C. Larock, *Org. Lett.*, 1999, **1**, 553–556; (*c*) Q. Huang, J. A. Hunter and R. C. Larock, *Org. Lett.*, 2001, **3**, 2973–2976; (*d*) K. R. Roesh and R. C. Larock, *J. Org. Chem.*, 2002, **67**, 86–94; (*e*) Q. Huang, J. A. Hunter and R. C. Larock, *J. Org. Chem.*, 2002, **67**, 3437–3444; (*f*) H. Zhang and R. C. Larock, *Tetrahedron Lett.*, 2002, **43**, 1359–1362.

8 For other isoquinoline formation from related intermediates, see: (*a*) P. N. Anderson and J. T. Sharp, *J. Chem. Soc., Perkin Trans. 1*, 1980, 1331–1334; (*b*) T. Sakamoto, Y. Kondo, N. Miura, K. Hayashi and H. Yamanaka, *Heterocycles*, 1986, **24**, 2311–2314; (*c*) T. Sakamoto, A. Numata and Y. Kondo, *Chem. Pharm. Bull.*, 2000, **48**, 669–772; (*d*) G. Dai and R. C. Larock, *Org. Lett.*, 2001, **3**, 4035–4038; (*e*) Q. Huang and R. C. Larock, *Tetrahedron Lett.*, 2002, **43**, 3557–3560; (*f*) N. Asao, S. Yudha S, T. Nogami and Y. Yamamoto, *Angew. Chem., Int. Ed.*, 2005, **44**, 5526–5528.

9 For the synthesis of isoquinolines by three-component reaction, see: (*a*) N. Asao, K. Iso and S. Yudha S, *Org. Lett.*, 2006, **8**, 4149–4151; (*b*) M. Oikawa, Y. Takeda, S. Naito, D. Hashizume, H. Koshino and M. Sasaki, *Tetrahedron Lett.*, 2007, **48**, 4255–4258.

10 Actually, one-portion addition of all the four components using **4j** gave a complex mixture of unidentified products without producing **6** (compare with Table 1, entry 10).

11 For isoquinoline formation with such ammonium salts as formate, carbonate, and ammonia, see ref. 8*c*.

12 In the reaction using **4i**, a hydrogen atom at the 4-position of **6a** would come from H_2O generated in imine formation.

13 At the present stage of our understanding, the reason for this unsatisfactory result is unclear.

Review:

AIDS: How Do We Overcome This Social or Biodisaster?

Tsutomu Murakami and Naoki Yamamoto

National Institute of Infectious Diseases
1-23-1 Toyama, Shinjuku-ku, Tokyo 162-8640, Japan
E-mail: tmura@nih.go.jp
[Received January 15, 2007; accepted January 22, 2007]

Some 40 million people in the world now live with the human immunodeficiency virus (HIV), which causes the acquired immunodeficiency syndrome (AIDS). The introduction of highly active antiretroviral therapy (HAART) has dramatically reduced AIDS mortality in developed countries, but problems with HAART itself, such as side effects and the emergence of the drug-resistant viruses. Despite tremendous effort to develop either a preventive or therapeutic AIDS vaccine, no effective ones have emerged despite promising candidate anti-HIV drugs as a back up for HAART. Given that, although not a curable, AIDS is preventable and controllable, it is urgent to disseminate effective HIV prevention and treatment to the virus-infected people all over the world in order to stop the global AIDS epidemic as soon as possible.

Keywords: HIV (human immunodeficiency virus), AIDS (acquired immunodeficiency syndrome), HAART (highly active antiretroviral therapy), host factors, vaccine

1. Introduction

Some 25 years have passed since the acquired immunodeficiency syndrome (AIDS) epidemic in the United Sates was first recognized with the publication in a report in *Morbidity and Mortality Weekly Report* [1]. Since then, 65 million people have reportedly been infected with the human immunodeficiency virus (HIV) and an estimated 25 million have died of AIDS [2, 3]. Although the introduction of combination of anti-HIV drugs so-called highly active antiretroviral therapy (HAART) in developed countries has dramatically reduced AIDS and AIDS-related disease mortality, HAART itself brings with it problems such as side effects of the drugs and the emergence of the drug-resistant viruses. The number of those newly infected and those dying AIDS continues to increase globally, especially in Africa. Health sectors in many affected countries face severe shortages of human and financial resources, while fighting to cope with the growing impact of AIDS [4]. This makes HIV infection and AIDS social or biodisaster in this era. In Japan alone, the accumulated number of HIV-infected people or developing AIDS reportedly exceeds 10,000 in 2005 [5]. Among developed countries, Japan is the only nation where the number of newly HIV-infected people continues to increase. Tremendous efforts should be done globally to overcome and stop this disaster. In this review, we briefly summarize the emergence and spread of the HIV/AIDS epidemic, and describe the efforts made against it, including basic virological research with special references to host factors, anti-HIV therapy, and HIV vaccines.

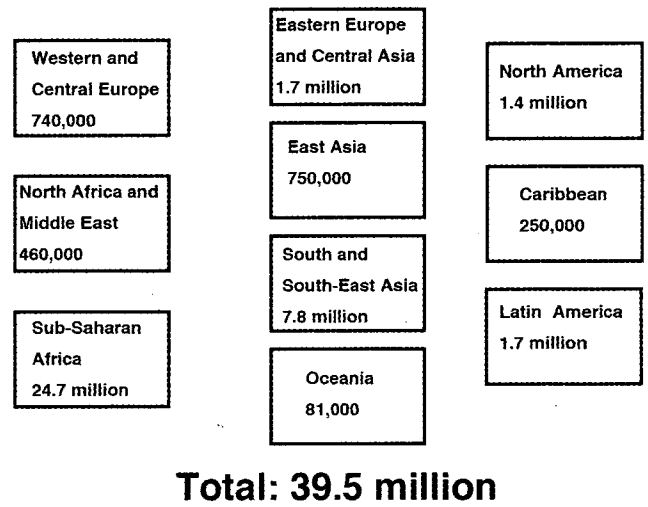

Fig. 1. People living with HIV in 2006 [6].

2. Global HIV/AIDS Epidemic

2.1. HIV Infection and AIDS Status

Today, 40 million people are living with HIV. Of these, an estimated 4.3 million people are newly infected and an estimated 2.9 million died of AIDS in 2006 alone [6]. Overall, the number of people living with HIV has continued to increase due to such factors as population growth and life-prolonging effects of antiretroviral therapy (ART) although HIV incidence as such appears to have been leveled off and stabilized since the late 1990s. Globally, those newly infected with HIV stand out among young populations of 15 to 24 years of age, who account for about 40% of new HIV infections among those 15 years and older. The sections that follow summarize main global and regional trends (**Fig. 1**) [6].

1) Sub-Saharan Africa

About 25 million people – globally, 63% of all persons with HIV – live in Sub-Saharan Africa. Despite great efforts to open access to ART, 2.1 million people died of AIDS during 2006. The HIV epidemic pattern varies with the country, increasing in some such as Mozambique, and South Africa, decreasing in prevalence among adults such as in Zimbabwe, or plateauing or declining as in East Africa. In West and Central Africa, the epidemic varies from country to country.

2) Asia

An estimated 8.6 million people – two thirds of them in India – were living with HIV in Asia in 2006. A major concern is the explosion of HIV/AIDS in China – the world's most populous nation –, and in India, the second most populous. About 1 million people in China reportedly have HIV. The major causes of HIV infection are unprotected paid sex and drug needle use in South and South-East Asia.

3) Eastern Europe and Central Asia

The AIDS epidemic continues in Eastern Europe and Central Asia, with the number of people with HIV expanding 20 times in the last 10 years. Of the 1.7 million living with AIDS, 270,000 people were newly infected in 2006. Use of non-sterilizing drug needles is the major cause of HIV transmission.

4) Latin America and the Caribbean

In Latin America, about 1.7 million live with AIDS, of whom 140,000 were newly infected during 2006. The region's biggest epidemic is with Brazil, which is home to more than one-third of those with HIV in Latin America. HIV infection is prevalent in men having sex with men, those injecting drugs, and commercial sex workers and their clients. The Caribbean countries have an estimated 250,000 people with AIDS in 2006, and AIDS is the primary cause of death among adults.

5) North Africa and the Middle East

In North Africa and the Middle East, an estimated 460,000 people, among whom 68,000 were newly infected with HIV in 2006. About 80% of them live in Sudan. Poor HIV surveillance makes it difficult to estimate what the major cause of prevalence is.

6) North America and Western and Central Europe

In North America and Western and Central Europe, 2.1 million – about two-thirds living in the United States – have AIDS, of whom 65,000 were newly infected during 2006. The total number of HIV-infected people in these two regions is increasing mainly due to the life-prolonging effects of ART. In the USA, the main risk factor for HIV infection is unsafe sex between men. Although the number of newly HIV-infected people in North America has plateaued, new HIV infection is increasing in Western Europe.

Many recommendations have been made to stop the HIV/AIDS pandemic, including the following strategy made by the 2006 report on the global AIDS epidemic by UNAIDS [7].

Provisions include:

1. Sustained and increased commitment and leadership
2. Sustained and increased financing
3. Aggressively addressing AIDS-related stigma and discrimination

Implementing these recommendations is imperative to stop the epidemic.

Commitment and action in the following areas are required for achieving universal access to treatment by 2010, adopted at the 2005 meeting of the G8 nations and the United Nations World Summit in 2005 [7]:

1) Strengthening AIDS prevention

HIV prevention and education should target to vulnerable groups, especially young people, including commercial sex workers, injecting drug users (IDUs), and men who having same gender sex.

2) Building treatment access

Expanded efforts are required to increase access to ART and to drugs that prevent opportunistic infections.

3) Strengthening human resources and organizations

The number of health-care workers and training facilities must be increased.

4) Ensuring available, affordable products for HIV prevention and treatment

Action must be increased to ensure the affordability of prevention and the availability of treatment, including condoms and antiretroviral drugs.

5) Investing in drug, microbicide, and vaccine R&D

Efforts must continue in developing new types of anti-HIV drugs, topical microbicides, and preventive vaccines.

2.2. HIV Infection and AIDS Status in Japan [5]

1) Reported number of HIV-infected people and AIDS patients

More than 10,000 people, mostly Japanese men, had HIV in 2005. Although HIV prevalence is low compared to most other countries, the reported number of new HIV sufferers was 832 in 2005 – the highest since surveillance started in 1985 (**Fig. 2**).

2) Route of infection

Same-gender male sex and heterosexual sex are the two major routes of infection in HIV-infected and AIDS patients in Japan. IDUs account for fewer than 1%, which is low compared to that of other countries, where IDUs usually exceeds 20%.

3) Age

HIV-infected people in Japan are concentrated among those 15-39 years of age, who account for 71% of the total. Those with AIDS, however, are mainly from 25 to 54 years old.

The percentage of AIDS patients among the HIV-infected is about 30%, suggesting that many patients are not diagnosed until they develop AIDS. This implies that many potential (unreported) people are infected with HIV. To reduce the number of those with HIV/AIDS in Japan, it is most important to strengthen prevention